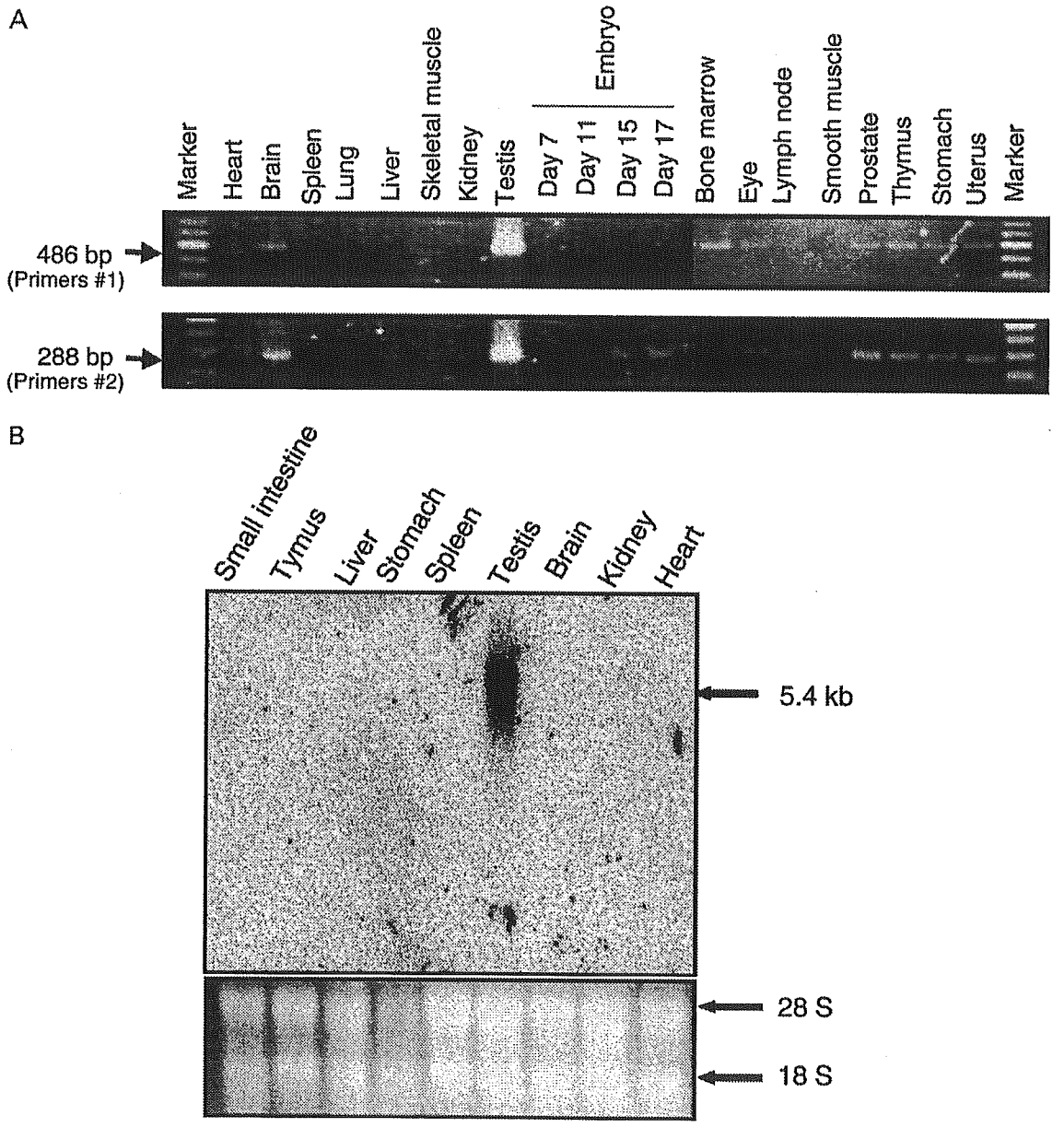

Fig. 5. Expression of the mouse *Abcc12* gene in different tissues. The Abcc12 transcript was detected by PCR (A) and by Northern hybridization (B) as described in Section 2. For the PCR detection (A), two sets of primers (#1 and #2; Fig. 1) were used. The resulting PCR products were 486 and 288 bp, as indicated by arrows. For the Northern hybridization (B), RNA (15 μg/lane) prepared from mouse tissues was fractionated by electrophoresis in 1.0% (w/v) agarose gels and visualized by ethidium bromide (bottom). 18S and 28S rRNAs are indicated by arrows. Northern hybridization (top) with a ^{32}P-labeled probe was carried out as described in Section 2. The detected Abcc12 mRNA (5.4 kb) is indicated by an arrow.

Abcc12 was observed in the testis. Relatively lower expression was detected in the brain, bone marrow, eye, lymph node, prostate, thymus, stomach, and uterus in the adult mouse. Northern blot hybridization (Fig. 5B) clearly demonstrates the predominant expression of mouse Abcc12 in the testis, being consistent with the results of RT–PCR (Fig. 5A). The transcript size of mouse Abcc 12 was about 5.4 kb.

3.5. Localization of mouse Abcc 12 in the testis

To elucidate the expression site of Abcc12 in the mouse testis, we have carried out laser-captured microdissection and RT–PCR. The seminiferous tubules and the interstitium were dissected, and RNA was extracted to prepare cDNA (see Section 2). PCR was carried out with the same primer

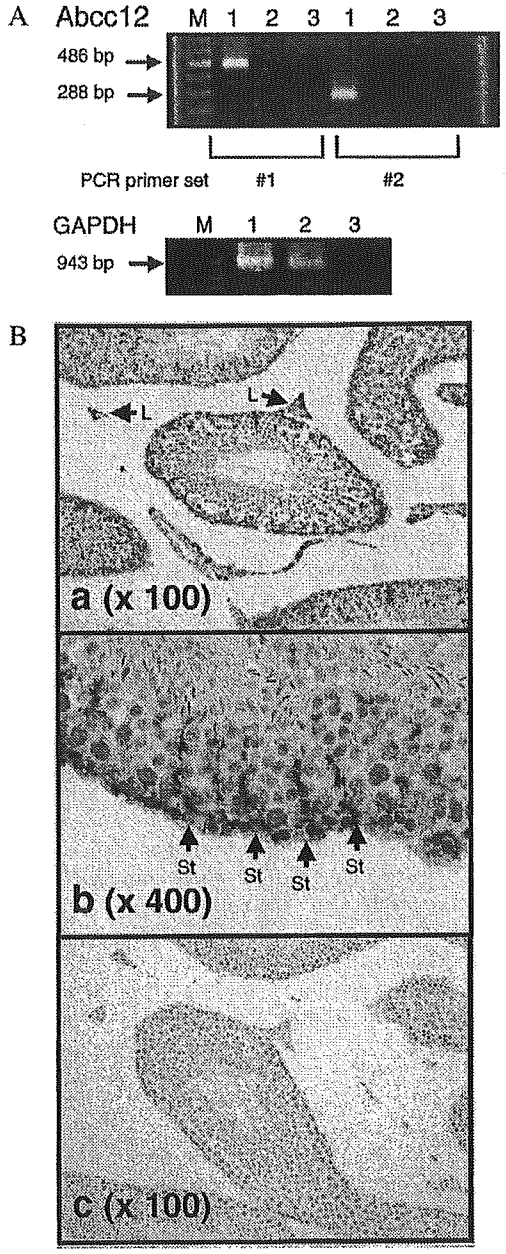

Fig. 6. Detection of the Abcc12 transcript in the mouse testis by means of laser-captured microdissection and RT–PCR (A) as well as by in situ hybridization (B). (A) Abcc12 and GAPDH transcripts were detected by PCR with RT reaction products prepared from micro-dissected samples. For the PCR detection, two sets of primers (#1 and #2; Fig. 1) were used, and the resulting PCR products were 486 and 288 bp, as indicated by arrows. The 943 bp product of GAPDH is the positive control for the PCR reaction. Lane M, DNA size markers; lane 1, seminiferous tubules; lane 2, stroma cells; lane 3, without RT reaction products. (B) The Abcc12 transcript in the mouse testis was detected by in situ hybridization as described in Section 2. Panels a and b show the results of hybridization with the anti-sense probe, whereas panel c shows the negative control, i.e. hybridization with the sense probe. Magnifications are indicated in parentheses. Arrows indicate Leydig (L) and Sertoli (St) cells.

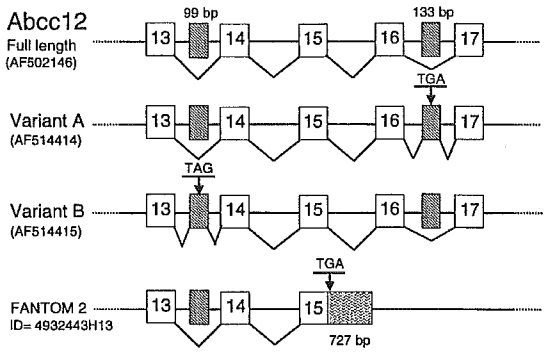

Fig. 7. Schematic illustration for alternative splicing of the *Abcc12* gene. Exons are numbered according to the sequence of the cloned Abcc12 cDNA. Variant A cDNA has one extra exon (133 bp) with a stop codon (TGA) between exons 16 and 17. Variant B cDNA has one extra exon (99 bp) with a stop codon (TAG) between exons 13 and 14. The exon 15 of the FANTOM 2 cDNA (ID = 4932443H13) has a 727 bp extension, as compared with the exon 15 of Abcc12 cDNA.

sets #1 and #2 as described above. As shown in Fig. 6A, Abcc12 expression was exclusively high in the seminiferous tubules, whereas little expression was detected in the interstitium. To gain further insight into cell type-specific expression of the *Abcc12* gene, we carried out in situ hybridization. Fig. 6B depicts the results of the in situ hybridization, demonstrating that the expression of Abcc12 was high in Sertoli cells of the seminiferous tubules (Fig. 6B, panel b). In addition, expression of Abcc12 was also detected in Leydig cells of the interstitium (Fig. 6B, panel a) under our hybridization conditions. No hybridization signal was observed with the sense probe, as the negative control (Fig. 6B, panel c).

3.6. Splicing variants of Abcc12

During the cloning of Abcc12 cDNA in the present study, we have discovered two variant forms of Abcc12 (GenBank accession numbers: AF514414 and AF514415 for variants A and B, respectively). Fig. 7 summarizes the configurations of those variants of the Abcc12 transcript together with the partial cDNA (ID = 4932443H13) reported in the FANTOM 2 database. The cDNAs of both variants A and B consist of 30 exons. As shown in Fig. 7, the variant A cDNA has an extra exon (133 bp) located between exons 16 and 17. Although the variant A cDNA consists of a total of 30 exons, the variant A is considered to encode a short peptide (775 amino acid residues), because the extra exon has a translation stop codon, TGA (Fig. 7). Likewise, the variant B cDNA has one extra exon (99 bp) with a stop codon (TAG) between exons 13 and 14 (Fig. 7), and, therefore, it also encodes a short peptide (687 amino acid residues). On the other hand, the FANTOM 2 cDNA (ID = 4932443H13) cloned by the 5′-oligo-cap method (Carninci et al., 1996) has an extension (121 bp) at the

5′-end of the cDNA, as compared with the cloned Abcc12 cDNA (data not shown). It is noteworthy that the exon 15 of the FANTOM 2 cDNA is different from that of the Abcc12 cDNA cloned in this study, although the other exons 2–14 are identical. Indeed, the exon 15 in the FANTOM 2 cDNA is 727 bp larger than the exon 15 of Abcc12 cDNA, but it encodes a translation stop codon (TGA) in the extended sequence (Fig. 7).

4. Discussion

4.1. Molecular characteristics of mouse Abcc12 cDNA

In the present study, we have cloned and characterized the cDNA of a new mouse ABC transporter, named Abcc12. The cloned cDNA was 4511 bp long and comprised a 4101 bp open reading frame. The deduced peptide consists of 1367 amino acid moieties, carrying two sets of Walker A, Walker B (Walker et al., 1982), and signature C (Higgins, 1992) motifs within the peptide (Fig. 2A). Based on the ATP binding cassettes and the putative trans-membrane spanning domains (Fig. 2B), Abcc12 is regarded as a 'full' ABC protein. The amino acid sequence of the Abcc12 protein deduced from the cloned cDNA exhibits the highest identity (84.5%) to human ABCC12 among all of the members of the ABCC subfamily hitherto identified in the human and the mouse (Table 1 and Fig. 3). Indeed, the hydropathy profile of mouse Abcc12 is virtually the same as that of human ABCC12 (Fig. 2B). From these results, it could be concluded that mouse Abcc12 is the orthologue of human ABCC12. In addition, our data suggest that the cDNA sequence of human ABCC12 (MRP9) recently reported by Bera et al. (2002) may be a splicing variant form, since exons 5 and 16 are missing in their sequence.

Based on the phylogenic relationship deduced from the amino acid sequence identities, the ABCC subfamily could be clustered into four classes (Fig. 3). For example, class A involves human ABCC1, ABCC2, ABCC3, and ABCC6, as well as mouse Abcc1, Abcc2, and Abcc6. These ABC transporters appear to function as conjugate transporters, e.g., GS-X pumps and/or multi-specific organic anion transporters (cMOAT) (Ishikawa, 1992; Borst and Oude Elferink, 2002). On the other hand, class B includes human ABCC8 (SUR1), ABCC9 (SUR2), and mouse Abcc9, which are sulfonylurea receptors coupled with potassium channels, i.e., Kir 6.1 or Kir 6.2. Human CFTR (ABCC7), ABCC10, mouse Abcc7 (mouse CFTR), and Abcc10 are involved in class C. Mutations in the *CFTR* gene are known to be the cause of cystic fibrosis, an autosomal recessive genetic disorder affecting a number of organs, including the lungs, airways, pancreas, and sweat glands (http://www.genet.sickkid.on.ca/cftr/). The physiological function of ABCC10 in this class is not known at the present time.

According to this clustering, the mouse Abcc12 belongs to class D, which involves human ABCC4, ABCC5, ABCC11, and ABCC12, as well as mouse Abcc4 and Abcc5 (Fig. 3). Recent studies demonstrated that human both ABCC4 and ABCC5 transport nucleotide analogues (Schuetz et al., 1999; Wijnholds et al., 2000; Jedlitschky et al., 2000; Chen et al., 2001). ABCC5 reportedly does not confer multidrug resistance when over-expressed in human embryonic kidney 293 cells (McAleer et al., 1999). Because of the similarity of the amino acid sequences, it is assumed that human ABCC11 and ABCC12 are functionally related to ABCC4 or ABCC5.

4.2. Mouse Abcc12 gene: an orthologue of human ABCC12 gene

Our conclusion that mouse Abcc12 is the orthologue of human ABCC12 is supported by similarities in the location and organization of those genes, as well. The present study provides evidence that the open reading frame in the mouse Abcc12 cDNA consists of 29 exons, as does the human ABCC12 cDNA (Yabuuchi et al., 2001; Tammur et al., 2001). In addition, the mouse *Abcc12* and human *ABCC12* genes (29 exons and introns) span 62 and 63 kb, respectively. The mouse *Abcc12* gene is located between two microsatellite markers, D8Mit347 and D8Mit348, on the chromosome 8D3 locus. This locus reportedly contains many conserved linkage homologies with human chromosome 16q12.1 (Serikawa et al., 1998), where the human *ABCC12* gene has recently been discovered (Yabuuchi et al., 2001; Tammur et al., 2001). Being consistent with this idea, the chromosomal location of the mouse *Siah 1* gene and its distance (167 kb) from the Abcc12 gene is conserved in the human chromosome 16q12.1 where both *SIAH 1* and *ABCC12* genes are located. The human *SIAH 1* gene (Hu et al., 1997) encodes a 282-amino-acid protein with 76% amino acid identity to the *Drosophila* SINA protein which is involved in the *ras* signaling pathway to mediate the R7 photoreceptor formation in the *Drosophila* eye (Carthew and Rubin, 1990). *Siah 1a* is one of the mouse orthologue genes and is mapped on the chromosome 8D3 locus (Holloway et al., 1997). Taken together, it is strongly suggested that the mouse *Abcc12* gene is closely related to the human *ABCC12* gene in terms of both the protein structure and the organization of the gene.

It is of importance, however, to note that in spite of the tandem location of both *ABCC11* and *ABCC12* genes on human chromosome 16q12.1, there was no mouse orthologue gene corresponding to the human *ABCC11* at that mouse chromosomal locus. In addition, there was no putative *Abcc11* gene detected even by an extensive search throughout the currently available mouse genome data. Thus, it appears that the *Abcc11* gene is absent from the mouse genome.

4.3. Tissue-specific expression of the mouse Abcc12 gene

We have previously reported that the expression of the

human *ABCC12* gene was widely distributed in various tissues, including testis, brain, liver, lung, kidney, thymus, prostate, ovary, colon, and leukocytes as well as in several fetal tissues (Yabuuchi et al., 2001). In contrast, the present study demonstrates that the mouse *Abcc12* gene is expressed at high levels exclusively in the testis (Fig. 5). The reason for such differences in organ-specific expression profiles between mouse Abcc12 and human ABCC12 is not known, but may be eventually explained by analysis of the promoter regions of those genes.

In the present study, by means of laser-captured microdissection combined with RT–PCR as well as in situ hybridization, the *Abcc12* transcript was detected in Sertoli cells of the seminiferous tubules in the mouse testis (Fig. 6A,B). In addition, in situ hybridization further revealed the expression of the *Abcc12* in Leydig cells, as well (Fig. 6B). Accumulating evidence suggests that the blood-testis barrier plays an important role in protecting the germ cells from harmful influences. To date it has been reported that ABCB1 (P-glycoprotein or MDR1) is expressed in luminal capillary endothelium and on the myoid-cell layer around the seminiferous tubule (Bart et al., 2002), whereas ABCC1 (MRP) is located basolaterally on both Sertoli and Leydig cells (Wijnholds et al., 1998). These ABC transporters are regarded as the first line players in the body's detoxification system. In this context, Abcc12 is also considered to play a role as a member of such a detoxification system, or it may be involved in the transport of endogenous substances in the testis. The physiological function and substrate specificity of Abcc12 remains to be elucidated.

4.4. Concluding remarks

Northern blot analysis revealed that mRNA with a size of 5.4 kb is the major transcript of mouse Abcc12 in the testis (Fig. 5B). In the present study, however, we have detected the existence of at least two splice variants for mouse Abcc12 (Fig. 7). In addition, the results of the FANTOM 2 project (The FANTOM Consortium, 2002) demonstrate that there is another splicing variant form that encodes a shorter peptide of Abcc12 (Fig. 7). These data suggests that mouse Abcc12 is transcribed into multiple forms by means of alternative splicing.

In the previous paper, we demonstrated that the human ABCC12 gene is transcribed into several splice variants (Yabuuchi et al., 2001). Recently, Bera et al. (2002) reported that the human ABCC12 (MRP9) is expressed as two major transcripts of 4.5 and 1.3, and that the 4.5 kb transcript is highly expressed in the epithelial cells of breast cancer. Transcript of the ABCC12 gene were detected in cell lines of carcinoma and adenocarcinoma originating from breast, lung, colon pancreas and prostate, as well (Yabuuchi et al., 2001), suggesting that expression of the ABCC12 gene may be up-regulated during carcinogenesis. Therefore, it is of great interest to study how alternative splicing is regulated in the expression of the human ABCC12 and mouse Abcc12 genes.

Acknowledgements

The authors thank Ms. Yukiko Saito (University of Tokyo Medical School) for her technical assistance in the preparation of tissue samples. This study was supported by research grants entitled 'Studies on the genetic polymorphism and function of pharmacokinetics-related proteins in Japanese population' (H12-Genome-026) and 'Toxicoproteomics: expression of ABC transporter genes and drug–drug interactions' (H14-Toxico-002) from the Japanese Ministry of Health and Welfare as well as by a Grant-in-Aid for Creative Scientific Research (No. 13NP0401) and a research grant (No. 14370754) from the Japan Society for the Promotion of Science. In addition, this study was supported, in part, by the institutional core grant of the 21st Century COE Program from the Ministry of Education, Culture, Sports, Science and Technology.

References

Bart, J., Groen, H.J.M., van der Graaf, W.T.A., Hollema, H., Hendrikse, N.H., Vaalburg, W., Sleijfer, D.T., de Vries, E.G.E., 2002. An oncological view on the blood-testis barrier. Lancet Oncol. 3, 357–363.

Bera, T.K., Lee, S., Salvatore, G., Lee, B., Pastan, I., 2001. MRP8, a new member of ABC transporter superfamily, identified by EST database mining and gene prediction program, is highly expressed in breast cancer. Mol. Med. 7, 509–516.

Bera, T.K., Iavarone, C., Kumar, V., Lee, S., Lee, B., Pastan, I., 2002. MRP9, an unusual truncated member of the ABC transporter superfamily, is highly expressed in breast cancer. Proc. Natl. Acad. Sci. USA 99, 6997–7002.

Borst, P., Oude Elferink, R., 2002. Mammalian ABC transporters in health and disease. Annu. Rev. Biochem. 71, 537–592.

Carninci, P., Kvam, C., Kitamura, A., Okazaki, Y., Kamiya, M., Shibata, K., Sasaki, N., Izawa, M., Muramatsu, M., Hayashizaki, Y., Schneider, C., 1996. High-efficiency full-length cDNA by biotinylated CAP trapper. Genomics 37, 327–336.

Carthew, R.W., Rubin, G.M., 1990. Seven in absentia, a gene required for specification of R7 cell fate in the Drosophila eye. Cell 63, 561–577.

Chen, Z.S., Lee, K., Kruh, G.D., 2001. Transport of cyclic nucleotides and estradiol 17-beta-D-glucuronide by multidrug resistance protein 4. Resistance to 6-mercaptopurine and 6-thioguanine. J. Biol. Chem. 276, 33747–33754.

Cole, S.P., Bhardwaj, G., Gerlach, J.H., Mackie, J.E., Grant, C.E., Almquist, K.C., Stewart, A.J., Kurz, E.U., Duncan, A.M., Deeley, R.G., 1992. Overexpression of a transporter gene in a multidrug-resistant human lung cancer cell line. Science 258, 1650–1654.

Dean, M., Rzhetsky, A., Allikmets, R., 2001. The human ATP-binding cassette (ABC) transporter superfamily. Genome Res. 11, 1156–1166.

Higgins, C.F., 1992. ABC transporters: from microorganisms to man. Annu. Rev. Cell Biol. 8, 67–113.

Holloway, A.J., Della, N.G., Fletcher, C.F., Largespada, D.A., Copeland, N.G., Jenkins, N.A., Bowtell, D.D., 1997. Chromosomal mapping of five conserved murine homologs of the Drosophila RING finger gene Seven-in-absentia. Genomics 41, 160–168.

Hu, G., Chung, Y.-L., Glover, T., Valentine, V., Look, A.T., Featon, E.R.,

1997. Characterization of human homologs of the Drosophila seven in absentia (sina) gene. Genomics 46, 103–111.

Ishikawa, T., 1989. ATP/Mg^{2+}-dependent cardiac transport system for glutathione S-conjugates: A study using rat heart sarcolemma vesicles. J. Biol. Chem. 264, 17343–17348.

Ishikawa, T., 1992. The ATP-dependent glutathione S-conjugate export pump. Trends Biochem. Sci. 17, 463–468.

Ishikawa, T., 2003. Multidrug resistance: genomics of ABC transporters. Encyclopedia of Human Genome, Nature Publishing Group, in press.

Jedlitschky, G., Burchell, B., Keppler, D., 2000. The multidrug resistance protein 5 functions as an ATP-dependent export pump for cyclic nucleotides. J. Biol. Chem. 275, 30069–30074.

Klein, I., Sarkadi, B., Varadi, A., 1999. An inventory of the human ABC proteins. Biochim. Biophys. Acta 1461, 237–262.

Kozak, M., 1991. An analysis of vertebrate mRNA sequences: intimations of translational control. J. Cell Biol. 115, 887–903.

Kyte, J., Doolittle, R.F., 1982. A simple method for displaying the hydropathic character of a protein. J. Mol. Biol. 157, 105–132.

Lee, W.-L., Tay, A., Ong, H.-T., Goh, L.-M., Monaco, A.P., Szepetowski, P., 1998. Association of infantile convulsions with paroxysmal dyskinesias (ICCA syndrome): confirmation of linkage to human chromosome 16p12–q12 in a Chinese family. Hum. Genet. 103, 608–612.

Leier, I., Jedlitschky, G., Buchholtz, U., Cole, S.p.C., Deeley, R.G., Keppler, D., 1994. The MRP encodes an ATP-dependent export pump of leukotriene C4 and structurally related conjugates. J. Biol. Chem. 269, 27807–27810.

McAleer, M.A., Breen, M.A., White, N.L., Matthews, N., 1999. pABC11 (also known as MOAT-C and MRP5), a member of the ABC family of proteins, has anion transporter activity but does not confer multidrug resistance when overexpressed in human embryonic kidney 293 cells. J. Biol. Chem. 274, 23541–23548.

Mouse Genome Sequencing Consortium, 2002. Initial sequencing and comparative analysis of the mouse genome. Nature 420, 520–562.

Müller, M., Meijer, C., Zaman, G.J., Borst, P., Scheper, R.J., Mulder, N.H., de Vries, E.G.E., Jansen, P.L.M., 1994. Overexpression of the gene encoding the multidrug resistance-associated protein results in increased ATP-dependent glutathione S-conjugate transport. Proc. Natl. Acad. Sci. USA 91, 13033–13037.

Saitou, N., Nei, M., 1987. The neighbor-joining method: a new method for reconstructing phylogenetic trees. Mol. Biol. Evol. 4, 406–425.

Schuetz, J., Connelly, M.C., Sun, D., Paibir, S., Flynn, P.M., Srinivas, R.V., Kumar, A., Fridland, A., 1999. MRP4: A previously unidentified factor in resistance to nucleoside-based antiviral drugs. Nature Med. 5, 1048–1051.

Serikawa, T., Cui, Z., Yokoi, N., Kuramoto, T., Kondo, Y., Kitada, K., Guenet, J.-L., 1998. A comparative genetic map of rat, mouse and human genomes. Exp. Anim. 47, 1–9.

Tammur, J., Prades, C., Arnould, I., Rzhetsky, A., Hutchinson, A., Adachi, M., Schuetz, J.D., Swoboda, K.J., Ptacek, L.J., Rosier, M., Dean, M., Allikmets, R., 2001. Two new genes from the human ATP-binding cassette transporter superfamily, ABCC11 and ABCC12, tandemly duplicated on chromosome 16q12. Gene 273, 89–96.

The FANTOM Consortium and the RIKEN Genome Exploration Research Group Phase I & II Team, 2002. Analysis of the mouse transcriptom based on functional annotation of 60,770 full-length cDNAs. Nature 420, 563–573.

Tomita, H., Nagamitsu, S., Wakui, K., Fukushima, Y., Yamada, K., et al., 1999. Paroxysmal kinesigenic choreoathetosis locus maps to chromosome 16p11.2–p12.1. Am. J. Hum. Genet. 65, 1688–1697.

Walker, J.E., Saraste, M., Runswick, M.J., Gay, N.J., 1982. Distantly related sequences in the α and β subunits of ATP synthetase, myosin, kinases and other ATP-requiring enzymes and a common nucleotide binding fold. EMBO J. 1, 945–951.

Wijnholds, J., Scheffer, G.L., van der Valk, M., van der Valk, P., Beijnen, J.H., Scheper, R.J., Borst, P., 1998. Multidrug resistance protein 1 protects the oropharyngeal mucosal layer and the testicular tubules against drug-induced damage. J. Exp Med. 188, 797–808.

Wijnholds, J., Mol, C.A., van Deemter, L., de Haas, M., Scheffer, G.L., Baas, F., Beijnen, J.H., Scheper, R.J., Hatse, S., De Clercq, E., Balzarini, J., Borst, P., 2000. Multidrug-resistance protein 5 is a multispecific organic anion transporter able to transport nucleotide analogs. Proc. Natl. Acad. Sci. USA 97, 7476–7481.

Yabuuchi, H., Shimizu, H., Takayanagi, S., Ishikawa, T., 2001. Multiple splicing variants of two new human ATP-binding cassette transporters, ABCC11 and ABCC12. Biochem. Biophys. Res. Commun. 288, 933–939.

Yabuuchi, H., Takayanagi, S., Yoshinaga, K., Taniguchi, N., Aburatani, H., Ishikawa, T., 2002. ABCC13, an unusual truncated ABC transporter, is highly expressed in fetal human liver. Biochem. Biophys. Res. Commun. 299, 410–417.

Int. J. Cancer: **104,** 147–154 (2003)

Publication of the International Union Against Cancer

OVEREXPRESSION OF CADHERINS SUPPRESSES PULMONARY METASTASIS OF OSTEOSARCOMA *IN VIVO*

Takeshi KASHIMA[1,2*], Kazuya NAKAMURA[1], Jitsutaro KAWAGUCHI[3], Masakatsu TAKANASHI[1], Tsuyoshi ISHIDA[4], Hiroyuki ABURATANI[5], Akira KUDO[3], Masashi FUKAYAMA[1] and Agamemnon E. GRIGORIADIS[2]

[1]*Department of Human Pathology, Graduate School of Medicine, University of Tokyo, Tokyo, Japan*
[2]*Department of Craniofacial Development, Guy's Hospital, King's College London, London, United Kingdom*
[3]*Department of Life Science, Tokyo Institute of Technology, Yokohama, Japan*
[4]*Department of Pathology, Tokyo University Hospital, University of Tokyo, Tokyo, Japan*
[5]*Genome Science Division, Research Center for Advanced Science and Technology, University of Tokyo, Tokyo, Japan*

Osteosarcoma by nature shows aggressive pulmonary metastasis; however, the underlying molecular mechanisms remain unclear. We previously showed that N-cadherin and cadherin-11 (OB-cadherin), which are highly expressed in normal osteoblasts, are anomalously expressed in human osteosarcoma (Kashima *et al.*, Am J Pathol 1999;155:1549–55). In the present study, we examined the role of cadherins in osteosarcoma metastasis using the mouse osteosarcoma cell line Dunn and its highly metastatic subline LM8. Oligonucleotide array and RT-PCR analyses demonstrated that Dunn and LM8 cells did not express appreciable levels of several members of the cadherin family, and Western blot analysis confirmed that Dunn and LM8 cells did not express P- cadherin, E- cadherin, N-cadherin or cadherin-11 protein. We therefore investigated the functional consequences of cadherin overexpression on cell migration and *in vivo* metastatic potential of LM8 cells. Several LM8 clones were isolated which expressed exogenous N-cadherin and cadherin-11 localized to the cell membrane and able to bind to β-catenin. Overexpression of N-cadherin or cadherin-11 in LM8 cells did not affect cell proliferation but caused an inhibitory effect on cell migration *in vitro*. *In vivo* analysis showed that N-cadherin- and cadherin-11-overexpressing cells exhibited a marked reduction in their ability to form pulmonary metastases, with significant decreases in lung weight and the number and weight of metastatic lesions, as well as the size and weight of primary lesions at the s.c.-inoculated site. These observations demonstrate that disruption of N-cadherin- and cadherin-11-mediated cell–cell adhesion is critical in the pulmonary metastasis of osteosarcoma.

Key words: *osteosarcoma; cadherin; osteoblast; lung; metastasis*

Osteosarcoma is a malignant bone-forming mesenchymal tumor and represents the most common primary tumor of bone.[1] Unlike other tumors, osteosarcomas usually arise in the extremities of teenagers and young adults. In addition to their aggressive growth, the worst problem of osteosarcomas is their high propensity to form pulmonary metastases. By the time diagnosis has been made, metastatic lesions have already developed in some cases. Progress over the past 2 decades in modern chemotherapy has improved the prognosis;[2] however, the morbidity is dependent on the existence of metastatic lesions and not on the primary tumor, and >40% of patients do not survive due to lung metastases.[3] Thus, understanding the molecular mechanisms underlying the pulmonary metastasis of osteosarcoma is essential for developing new methods of diagnosis, assessment and effective therapy.

Metastasis is the final step in the process of multistep tumorigenesis of malignant tumors.[4] This complex process is composed of 4 steps: initial cell detachment from the primary tumor, migration through the local stroma to the circulation, passage through the bloodstream and finally colonization of distant organs. During the above process, the primary tumor disrupts the tissue architecture, which is composed of extracellular matrix (ECM), and cells and is regulated by cell adhesion molecules (CAMs) and extracellular proteases. Any changes in the local surroundings are also transferred through the cytoplasmic domain of CAMs, and appropriate genes related to apoptosis, growth, migration and differentiation are activated or repressed to maintain tissue homeostasis. For instance, turnover of matrix is dependent on matrix-degrading proteases and urokinase, while cell–cell or cell–matrix interactions are controlled by cadherins, CD44, selectins, integrins or the proteins of the immunoglobulin superfamily. The metastatic and invasive phenotypes of tumors are associated with alterations in the binding specificities of CAMs and activation of extracellular proteases.[5]

Cadherins modulate calcium ion-dependent cell–cell adhesion and are important in cell aggregation, migration and sorting.[6] They mediate homophilic adhesion through their extracellular domains, and only cadherins of the same type can bind to each other, with the exception of the interaction between N-cadherin and R-cadherin. To date, more than 20 types of classic cadherin have been isolated, forming a large cadherin family.[7] Cadherins exhibit a tissue-specific pattern of expression: *e.g.*, E-cadherin is expressed in epithelia and expression of M-cadherin is restricted to muscle, whereas N-cadherin and cadherin-11 are widely expressed in mesenchymal and neural cells. Hence, cadherins are important in cell sorting during embryogenesis and for cell–cell communication to maintain adult tissue.[6] Cadherin function is controlled by the cytoplasmic tail.[8] It can interact with p120ctn and β-catenin or plakoglobin (γ-catenin), which are essential for cadherin-mediated cell adhesion. β-catenin binds to α-catenin, which further interacts with α-actinin, vinculin, ZO-1 and the actin cytoskeleton. Phosphorylation of both β-catenin and p120ctn causes dissociation from cadherins. Cadherin complexes are condensed at adherens junctions and play an important role in not only the regulation of cell–cell adhesion but also signal transduction.[9]

E-cadherin suppresses metastasis in many kinds of tumors.[10] In many carcinomas, expression of E-cadherin is correlated with tumor grade.[11] Invasive and metastatic, poorly differentiated car-

Grant sponsor: Canon Europe Foundation; Grant sponsor: Ministry of Education, Science and Culture of Japan; Grant sponsor: Vehicle Racing Commemorative Foundation; Grant sponsor: Department of Orthodontics and Paediatric Dentistry, King's College London, Guy's Hospital.

Dr. Ishida's current address is: Department of Pathology, Faculty of Medicine, Tokyo Medical University, Tokyo, Japan.

*Correspondence to: Department of Craniofacial Development, King's College London, Guy's Hospital, Tower Floor 28, London Bridge, London, SE1 9RT, UK. Fax: +44-(0)207-955-2704.
E-mail: kashima-tky@umin.ac.jp

Received 23 May 2002; Revised 21 October 2002; Accepted 23 October 2002

DOI 10.1002/ijc.10931

cinomas often lose or diminish their expression of E-cadherin, while less invasive, well-differentiated carcinomas retain E-cadherin expression. Both *in vitro* and *in vivo* studies have shown that cadherin-mediated cell–cell adhesion is important to suppress tumor invasion and further metastasis. In addition, abnormalities in not only cadherins but also their modulators lead to disruption of cell adhesion. Mutation of either β-catenin in gastric cancer cell lines or p120ctn in a colon cancer cell line alters cell–cell adhesion even when E-cadherin function is conserved, and overexpression of the normal proteins can rescue cell adhesion in these cells.[12,13] β-catenin also plays an important role in the Wnt signaling pathway, which is important in cell growth, mobility, differentiation and tumor formation.[14]

Bone homeostasis is controlled by the balance between resorption by osteoclasts and new formation by osteoblasts.[15] As in other organs, the importance of CAMs in bone cells has been well established. Normal osteoblasts display a coordinated sequence of proliferation and differentiation, and this is mediated not only by humoral factors but also by cell-surface receptors including CAMs.[16] Osteoblasts line bone surfaces and are linked to each other by adherens junctions, which are formed with cadherin complexes. We and others have previously reported that osteoblasts express several classes of cadherins, including *E-cadherin, N-cadherin, K-cadherin, R-cadherin* and *cadherin-11,* which are detected by RT-PCR; however, only N-cadherin and cadherin-11 are expressed at the protein level.[17–21]

Cadherin-11 is identical to *OB-cadherin,* which was cloned from the MC3T3-E1 mouse osteoblast cell line and has approximately 60% amino acid homology to *N-cadherin.*[22–24] Its structure is highly conserved among species, and there is 98% identity at the amino acid level between mouse and human.[22] *Cadherin-11* is highly expressed in the sclerotome during embryogenesis[23,24] as well as in osteoblastic cell lines and plays an important role in osteoblast differentiation.[18] For example, cadherin-11 null mice show an osteomalacia-like hypomineralization of long bones,[25] and dominant-negative cadherin inhibits osteoblast differentiation through disruption of cadherin function.[19,20] Hence, N-cadherin and cadherin-11 coordinately regulate the function and differentiation of osteoblasts.

We have previously studied cadherin expression in human osteosarcomas and have shown an abnormality in the expression of specific cadherins.[26] Expression of N-cadherin is highly suppressed and could not be detected at the protein level. The intact form of *cadherin-11* is also suppressed in osteosarcoma due to high expression of the alternatively spliced variant *cadherin-11,* resulting in a truncated cytoplasmic domain which does not participate in cell–cell adhesion.[17] In addition, a secreted form of cadherin-11 is the most abundant, which is generated by proteolysis and may disrupt the cell–cell adhesion of intact cadherin-11. In view of these data, we have hypothesized that downregulation of cadherin function in osteosarcoma is related to its morphology and metastatic potential.[26] These observations also prompted us to study the importance of these 2 cadherins in the formation of pulmonary metastasis of osteosarcomas *in vivo.* Here, we have profiled the cadherin expression pattern in Dunn osteosarcoma cells and the highly metastatic subline LM8 and examined whether cadherin function is related to pulmonary metastasis *in vivo.*

MATERIAL AND METHODS

Cell lines and antibodies

The mouse osteosarcoma cell line Dunn and its highly metastatic cell line LM8 were gifts from Dr. T. Ueda (Department of Orthopedic Surgery, Graduate School of Medicine, Osaka University, Osaka, Japan). LM8 cells were derived following 8 passages of Dunn cells *in vivo* according to the methods of Fidler, as described by Asai *et al.*[27] In brief, the parental cell line Dunn, which does not show spontaneous metastasis, was injected into the tail vein, and primary cultures obtained from the occasional pulmonary metastases were reinjected for a total of 8 times. The resulting cell population, designated LM8, invariably shows not only pulmonary metastasis but also spontaneous metastasis when inoculated s.c. All tumor cells were maintained in Eagle's MEM with nonessential amino acids (GIBCO BRL, Gaithersburg, MD) with 10% FCS (Trace Scientific, Castle Hill, Australia). The A431 human squamous cell carcinoma cell line (obtained from Dainihon Seiyaku, Osaka, Japan), as well as Itk$^-$ mouse cells and the N-cadherin or cadherin-11 transfectants LN2 and L7, respectively, were maintained in DMEM (GIBCO BRL) and 10% FCS.[22] All cell lines were maintained at 37°C in an incubator containing 5% CO_2. Polyclonal antibodies against N-cadherin and P-, E- and N-cadherin were purchased from Santa Cruz Biotechnology (Santa Cruz, CA) and Takara Shuzo (Shiga, Japan), respectively. OLA-9, a monoclonal antibody (MAb) against cadherin-11, was raised in cadherin-11 null mice using the recombinant extracellular domain 1 as an antigen.[18] The MAb against β-catenin was purchased from Transduction Laboratories (Lexington, KY).

Extraction of total RNA

Total RNA from cultured cells and an E17 mouse embryo was prepared using Trizol (GIBCO BRL) following the manufacturer's instructions.

High-density oligonucleotide array analysis

Total RNA (100 μg) from LM8 and Dunn cells was used to synthesize approximately 100 mg of cRNA and labeled with biotin by T7 RNA polymerase. The cRNA was hybridized to the high-density oligonucleotide array (Murine Genome Array U74A; Affymetrix, Santa Clara, CA), and the arrays were washed, stained and scanned using a Fluidics Station 400 (Affymetrix) and Hewlett-Packard (Palo Alto, CA) scanner as described previously.[28] The intensity of each feature of the array was calculated using Affymetrix Gene Chip software version 3.3. In calculating the change of average difference, normalization for all probe sets was performed and the fold change between the hybridization intensity of Dunn and LM8 samples was obtained.

RT-PCR and Southern blot analyses

Single-stranded cDNA was generated from 1 μg of total RNA and oligo dT primer, using Superscript II RnaseH$^-$ reverse transcriptase (GIBCO BRL). The sequence of the primers was previously described.[18] In brief, PCR for each class of cadherin was carried out for 22 cycles to avoid saturation; products were separated on a 1.2% agarose gel and transferred to a nylon membrane (Biodyne, East Hills, NY). Each PCR product was detected by probing desired digoxigenin (DIG)–labeled probes using the DIG Luminescent Detection Kit for Nucleic Acids (Roche, Indianapolis, IN).

Western blot analysis

Cells were lysed in TNE buffer containing 2% NP40, 20 mM TRIS (pH 8.0), 150 mM NaCl, 5 mM EDTA, 2 mM NaN_3, 0.1 mM PMSF, 2 μg/ml leupeptin and 20 μg/ml aprotinin. Tumor samples (0.5 g, s.c.) were thawed and washed twice in cold PBS. After cutting into small pieces and homogenization, samples were lysed in 1 ml of cold TNE buffer. Following incubation for 30 min at 4°C with a rotor mixer and centrifugation at 13,000 *g* for 20 min, supernatants were recovered. The protein concentration was measured by the Bradford method (Bio-Rad, Hercules, CA). A half-volume of 3× Laemmli sample buffer was added to 20 μg of each sample and boiled at 95°C for 5 min. After separation by 7.5% SDS-PAGE, proteins were electrophoretically blotted onto an Immobilon-P membrane (Millipore, Bedford, MA). Membranes were blocked with 5% BSA and incubated with primary antibody and horseradish peroxidase–labeled secondary antibody (Dako, Glostrup, Denmark). The immunoreactive signal was detected by the enhanced chemiluminescence system (Amersham, Aylesbury, UK).

Immunoprecipitation

Immunoprecipitation was carried out as previously described.[17] In short, cell proteins were solubilized in lysis buffer containing 0.5% NP40, 10 mM TRIS (pH 7.4), 150 mM NaCl, 1 mM EDTA, 1 mM EGTA, 0.2 mM sodium vanadate and protease inhibitors as described above. Supernatants were collected after centrifugation, and 2.5 μg of anti-β-catenin antibody and protein A-Sepharose were added to the samples at 4°C for 1 hr. Precipitates were boiled with Laemmli sample buffer and used for Western blotting as described above.

Transfection

Transfection of mouse N-cadherin or human intact form cadherin-11 cDNA into LM8 cells was performed as described previously.[17] In brief, *N-cadherin* or *cadherin-11* cDNA was cloned into pCXN2, an expression vector driven by a chicken β-actin-promoter and human cytomegalovirus enhancer, at EcoRI or XhoI sites, respectively.[29] Following transfection using Lipofectamine plus reagent (GIBCO BRL), stable transfectants were selected in 400 μg/ml G418 (Geneticin, GIBCO BRL).

Immunofluorescence

Cells were cultured on coverslips and fixed with 4% paraformaldehyde in PBS. Following permeabilization with 0.5% Triton X-100 and blocking with 5% BSA in PBS, coverslips were incubated with primary antibody and FITC-labeled secondary antibody (Dako). The immunoreactive signal was viewed using a Zeiss (Thornwood, NY) Axiophot microscope.

Growth properties of tumor cells in vitro

Cells were plated in a 6-well plate (5,000/well) on day 0 and cultured in MEM supplemented with 10% FCS. The total cell number was determined for 5 days using a hemocytometer.

In vitro *cell migration assay*

Cell motility was estimated in a Boyden chamber, with assays repeated a minimum of 3 times.[30] Culture inserts with 8 μm pore polyethylene terephthalate filters (3053; Becton Dickinson Labware, Franklin Lakes, NJ) were used in a 6-well plate. Serum-free conditioned medium from LM8 cells was used as a chemoattractant in the lower compartment. Cells (5×10^5) suspended in 500 μl of MEM with 0.1% BSA were added in the upper compartment. After 24 hr incubation, cells on the upper surface of the pore filter were removed by cotton swabs. Cells that penetrated the pore filter were stained with Diff-quick (Baxter, Deerfield, IL) and counted microscopically in 10 fields at ×100 magnification.

In vivo *pulmonary metastasis assay*

Male 5-week-old inbred C3H mice were used to create 7 study groups for 5 cadherin transfectants and 2 controls ($n = 4$–7). To estimate the *in vivo* metastatic potential to the lung, 10^7 trypsinized tumor cells were suspended in 1 ml MEM and injected s.c. into the back of the mice. Four weeks following inoculation, mice were killed and the size and weight of the lungs and s.c. tumors measured. Half of the s.c. tumor was snap-frozen in liquid nitrogen and stored at −80°C for further analysis. Following fixation in neutral buffered formalin, lungs were cut into 3 sections at their maximum dimensions. Paraffin-embedded specimens were cut 4 μm thick and stained with hematoxylin and eosin. The total number of lung metastases was counted microscopically.

Immunohistochemistry

Paraffin-embedded tissues were cut into 4 μm thick sections. Immunohistochemical studies were performed by the peroxidase avidin-biotin method with a VECTOR-elite ABC kit (Vector, Burlingame, CA). Antibodies against N-cadherin and cadherin-11 were applied after antigen retrieval in citrate acid buffer (pH 7.0 and 6.5, respectively). Substitution of primary antibodies by normal serum was used as a negative control.

Statistical analysis

All data were compared with controls using Dunnett's *post-hoc* test. All p values are 2-sided, with statistical significance set at $p < 0.05$.

RESULTS

Expression of cadherins in Dunn and LM8 cells

We initially screened the expression of different members of the cadherin family in both Dunn and LM8 cell lines by oligonucleotide array. On the arrays, there are 11 types of classic cadherin gene (Table I). Average differences in the cadherin family were up to 3.5-fold between Dunn and LM8 cells; however, these data were difficult to interpret because the signal intensity was below background level. Of the data which were above background, average differences between *E-cadherin* and *P-cadherin* were 1.2- and 1.4-fold, respectively, and they are expressed at slightly higher levels in LM8 compared to Dunn cells.

To verify the oligonucleotide array expression data, 8 different cadherin members were amplified in Dunn and LM8 cells by RT-PCR (Fig. 1*a*). Expression of *E-cadherin*, *N-cadherin* and *P-cadherin* was detected in both cell lines but at very low levels. Moreover, expression of *P-cadherin* was slightly higher in LM8 than in Dunn cells, consistent with the array data, and *N-cadherin* was also expressed at higher levels in LM8 cells (Fig. 1*a*). Other cadherin family members, including *R-cadherin*, *K-cadherin*, *cadherin-8*, *cadherin-11* and *M-cadherin*, were not expressed in either cell line. These data suggest that endogenous cadherin RNA levels are very low or absent in these 2 cell lines.

TABLE I – CADHERIN EXPRESSION PROFILING BY OLIGONUCLEOTIDE ARRAYS

	Average Difference		Fold change	Accession number
	Dunn	LM8		
E-cadherin (Cdh1)	228	276	1.2	X60961
N-cadherin (Cdh2)	3	−9	(−2.4)	M31131
P-cadherin (Cdh3)	92	126	1.4	X06340
R-cadherin (Cdh4)	−117	−138	(−3.5)	X69966
K-cadherin (Cdh6)	24	33	−1.1	D82029
Cadherin-8 (Cdh8)	−7	−10	(−1.7)	X95600
T1-cadherin (Cdh9)	25	23	−1.1	U69136
T2-cadherin (Cdh10)	12	−8	(−3.5)	U69137
OB-cadherin (Cdh11)	16	18	1.1	D21253
M-cadherin (Cdh15)	20	−10	(−1.9)	AJ245402
Ksp-cadherin (Cdh16)	−12	−9	(−1.4)	AF016271
β-Actin	1,175	1,042	−1.1	M12481

Cadherin expression profiling in Dunn and LM8 cells was carried out with high-density oligonucleotide arrays (Affymetrix, MU74A). Under Fold change, (−) indicates reduced expression in LM8 cells. Numbers in parentheses indicate that the signal intensity was not significant above background. The intensity of expression signals is presented as an average difference, which is the difference of signal intensity between antisense probes and missense probes with mismatch.

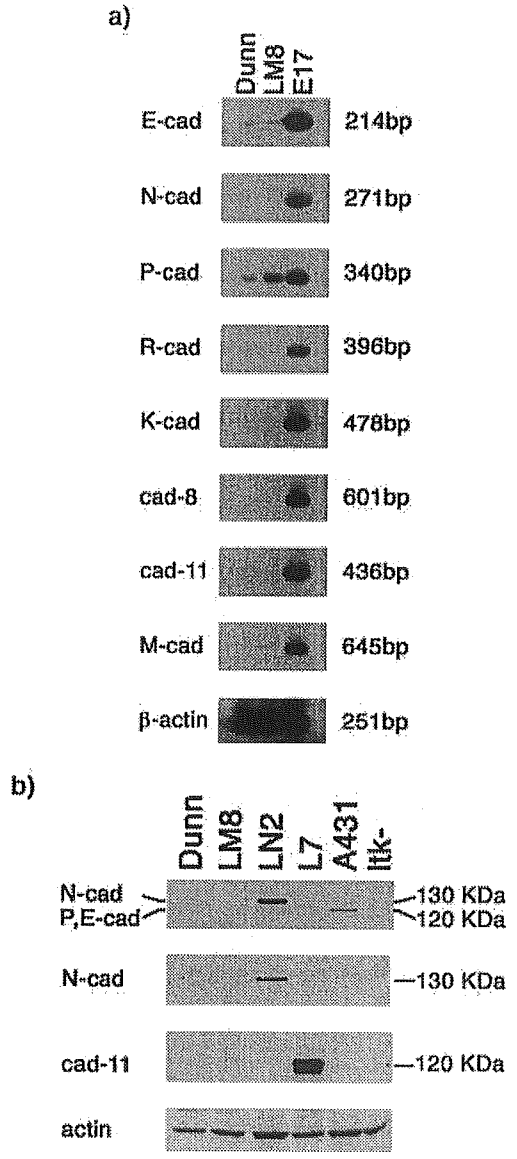

FIGURE 1 – Cadherin expression profiling in Dunn and LM8 cells. *(a)* RT-PCR/Southern blot analysis was performed using specific primer pairs for the indicated cadherin molecules. PCR was carried out for 22 cycles, to avoid saturation. cDNA from a 17-day-old mouse embryo (E17) was used as a positive control. PCR product sizes for each cadherin are indicated. *(b)* Western blot analysis of cadherin protein expression. Protein extracts were prepared from the indicated cell lines, and Western blotting was performed as described in Material and Methods using specific antibodies against P-/E-/N-cadherin, N-cadherin and cadherin-11 and actin as a loading control. LN2 and L7 cells are stable transfectants of Itk$^-$ fibroblasts overexpressing N-cadherin and cadherin-11, respectively. Protein sizes are indicated.

To confirm these results, we also examined the expression of some cadherins using specific antibodies and Western blotting (Fig. 1*b*). Expression of P- cadherin, E- cadherin, N-cadherin and cadherin-11 was not detected in either Dunn or LM8 cells. Similarly, Itk$^-$ fibroblasts did not express these cadherins, though the transfected clones LN2 and L7, which overexpress N-cadherin and cadherin-11, respectively, showed expression of N-cadherin and cadherin-11 as positive controls. A431 cells also express P- and E-cadherin, consistent with previous reports.[31]

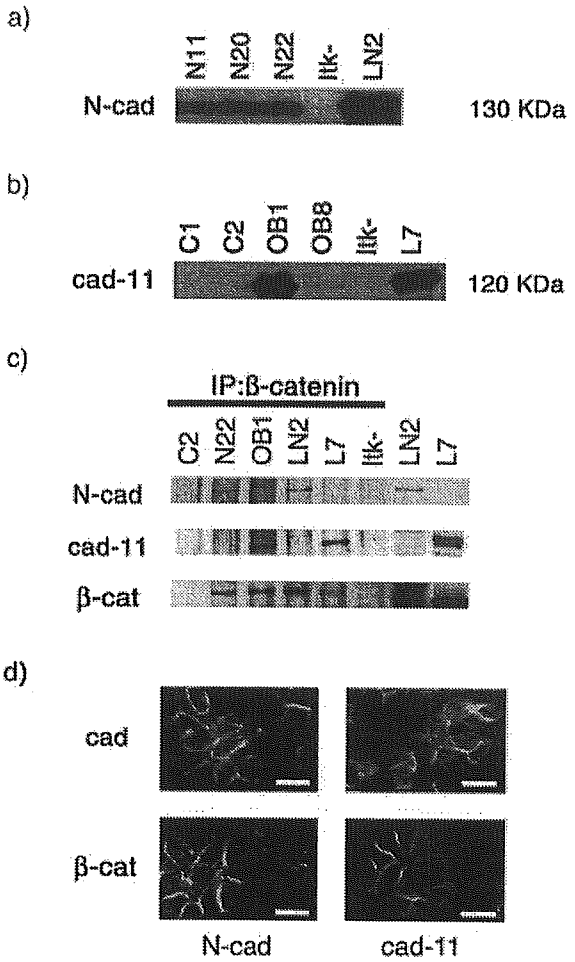

FIGURE 2 – Expression of exogenous cadherin proteins in LM8 transfectants. LM8 cells overexpressing either N-cadherin (N11, N20 N22) or cadherin-11 (OB1, OB8) were subjected to Western blotting using specific antibodies against *(a)* N-cadherin or *(b)* cadherin-11. C1, C2 and LN2, L7 cells are negative and positive control transfectants, respectively. Protein sizes are indicated. *(c)* Immunoprecipitation analysis of representative clones using an anti-β-catenin antibody followed by Western blotting for N-cadherin, cadherin-11 and β-catenin indicates specific cadherin–catenin complex formation in the different transfectants. The right 2 lanes are controls without immunoprecipitation. *(d)* Immunofluorescence staining of cells overexpressing N-cadherin (N-cad) or cadherin-11 (cad-11), with antibodies against N-cadherin (upper left), cadherin-11 (upper right) or β-catenin (lower panels). Bar = 100 μm.

Overexpression of cadherins

Since there was little endogenous expression of cadherins, we introduced *N-cadherin* and *cadherin-11* cDNAs into LM8 cells to investigate their function. After selection with G418, we obtained several clones. Western blot analysis demonstrated exogenous N-cadherin expression in clones LM8-N11, LM8-N20 and LM8-N22 (Fig. 2*a*). Exogenous cadherin-11 expression was also high in

LM8-OB1 cells, whereas LM8-OB8 cells expressed lower levels (Fig. 2*b*). Control clones (C1 and C2) transfected with empty vector failed to express cadherin-11 (Fig. 2*b*) or N-cadherin (data not shown). To verify the potential functionality of the exogenous cadherins, we next analyzed their ability to bind to β-catenin. Immunoprecipitation with an anti β-catenin antibody, followed by Western blotting for N-cadherin and cadherin-11, showed that these overexpressed cadherins complexed with β-catenin (Fig. 2*c*). Moreover, immunofluorescence analysis revealed that these cadherins and endogenous β-catenin are localized to the cell surface (Fig. 2*d*), which suggests that exogenous cadherins function as potent cell–cell adhesion molecules.

Cell proliferation and cell migration in vitro

We next investigated whether introduction of N-cadherin and cadherin-11 into LM8 cells would affect their growth properties and their capacity for invasion and motility. Growth curve analysis using each transfectant indicated that growth rates were similar between the parental cells and each clone (Fig. 3*a*). The reduced cell density in the control C1 clone may reflect slight variations in plating efficiency in the presence of G418. Further, analysis of *in vitro* migration indicated that compared with the 2 control transfectants, C1 and C2, the parental LM8 cells and all cadherin transfectants showed significantly less motility (Fig. 3*b*). These data suggest that overexpression of N-cadherin or cadherin-11 does not affect cell proliferation but appears to suppress the motility of LM8 clones *in vitro*.

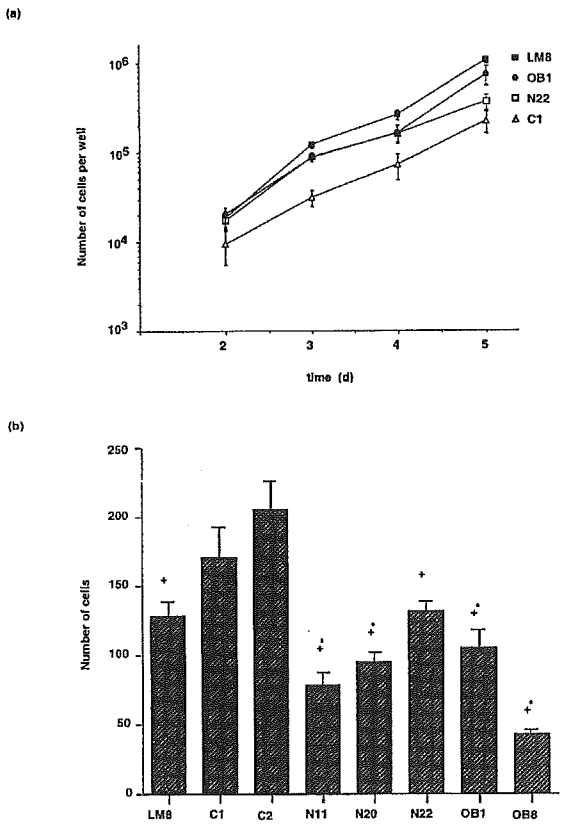

FIGURE 3 – *In vitro* analysis of cadherin transfectants. *(a)* Growth curve analysis of parental LM8 cells and representative cadherin transfectants. Data represent means ± SD of the number of cells/well. *(b) In vitro* migration potential of cadherin transfectants. Cell lines were plated on uncoated membranes with an 8 μm pore size and cultured. After 24 hr, cultures were stained and the number of cells migrating through the membrane was determined by averaging 10 fields of view at ×100 magnification. Data represent means ± SEM and were analyzed using Dunnett's *post hoc* test. * and + indicate statistical significance ($p < 0.05$) compared to C1 and C2, respectively.

In vivo *metastasis assay*

To clarify the role of N-cadherin and cadherin-11 in osteosarcoma metastasis *in vivo,* we inoculated these transfectants into C3H mice. After 4 weeks, all injected tumor cells formed large primary tumors at the injection site (see below). Upon examination of the lungs, marked differences were observed. Whereas a high number of metastatic lesions were observed in lungs of mice injected with control, empty vector–transfected cells, there was a marked reduction in metastases produced by cells overexpressing either N-cadherin or cadherin-11 (Fig. 4*a–f*). Expression of transfected genes was detected by immunohistochemistry both in the primary tumors (Fig. 4*g–i*) and in the lung metastases (Fig. 4*j–l*). Transgene expression was also confirmed by Western blot analysis of protein samples isolated from primary tumors (Fig. 4*m*).

Finally, we investigated whether the observed histologic differences could be confirmed by quantitative analysis. Measurements of the weight and volume of primary tumors at the injection site demonstrated a general inhibition of these parameters in tumors induced by N-cadherin- and cadherin-11-overexpressing cells compared to mock-transfected cells (Fig. 5*a,b*). Analysis of lung tissues revealed reduced total lung weight in mice harboring cadherin-overexpressing cells (Fig. 5*c*). In addition, the number of lung metastases was significantly reduced in all N-cadherin and in 1 cadherin-11 transfectant (Fig. 5*d*). LM8-OB8, which weakly expressed exogenous cadherin-11, showed no statistical differences in the number of metastases compared to control; however, metastatic foci were as small as in the other cadherin transfectants (data not shown). These observations are consistent with the reduction in lung weight. Thus, these data demonstrate that overexpression of cadherins attenuates the ability of osteosarcoma cells to form lung metastases.

DISCUSSION

In our study, overexpression of N-cadherin and cadherin-11 inhibited migration of osteosarcoma cells *in vitro* and suppressed their ability to form lung metastases in an *in vivo* spontaneous metastasis model. Both cadherins are highly expressed in normal osteoblasts and play important roles in osteoblast differentiation and cell–cell adhesion.[17–21] Moreover, we have previously demonstrated that expression of these cadherins is altered in human osteosarcoma.[26] Preliminary expression profiling by oligonucleotide arrays of the Dunn osteosarcoma cell line and its highly metastatic derivative LM8 indicated very few changes in the expression of a wide range of cadherin molecules. These results suggest that the enhanced metastatic potential of LM8 cells was not dependent on altered cadherin expression, and we are currently analyzing further the oligonucleotide array data to identify other genes that may be related to the pulmonary metastasis of osteosarcoma cells. Levels of *E-*, *P-* and *N-cadherin* were very low by RT-PCR analysis, and Western blotting confirmed that neither Dunn nor LM8 cells expressed detectable protein levels of these classical cadherins, including cadherin-11. Thus, LM8 osteosarcoma cells were ideal candidates for analyzing the functional consequences of overexpression of N-cadherin and cadherin-11 on their ability to form lung metastases. Exogenous cadherins were stably expressed in LM8 transfectants, and this was confirmed by immunolocalization studies. *In vitro* aggregation assays, which are commonly used to show cadherin-mediated cell–cell adhesion,[6,17] could not be carried out since LM8 and its subclones exhibited very strong adherence to the tissue culture substrate, which prevented the efficient preparation of a single-cell suspension in the

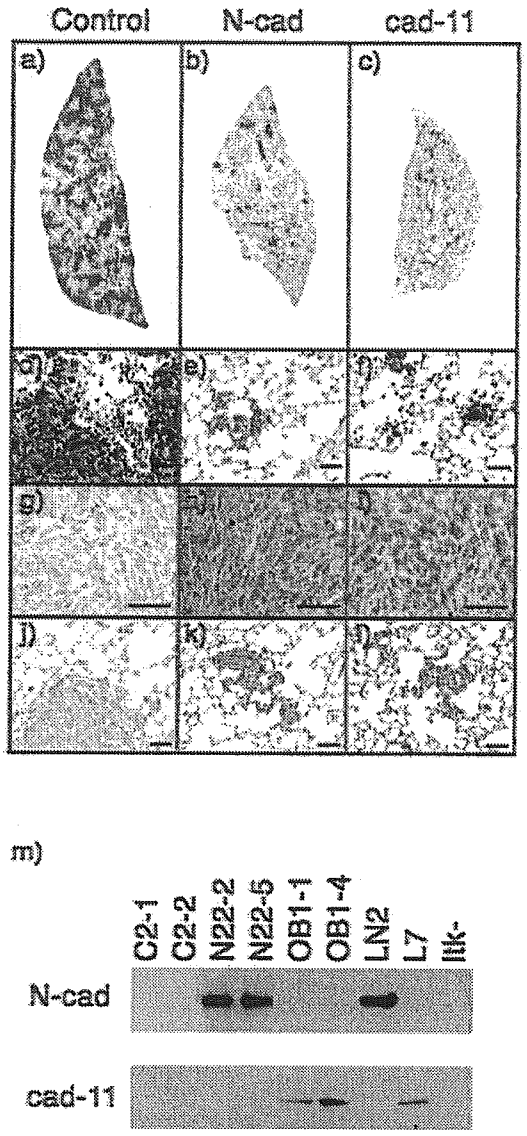

FIGURE 4 – *In vivo* metastasis of LM8 transfectants. Control *(a,d,g,j),* N-cadherin *(b,e,h,k)* and cadherin-11 *(c,f,i,l)* transfectants were injected s.c. into the backs of male C3H mice (n = 4–7), and lungs were fixed and processed after 4 weeks for analysis of metastases. Histologic analysis showing low *(a–c,* loupe view) and high *(d–f)* magnification micrographs of lungs from representative mice. Immunohistochemical analysis of primary tumors *(g–i)* and lung metastases *(j–l)* revealed that exogenous cadherins were expressed *in vivo. (m)* Western blot analysis of N-cadherin and cadherin-11 protein expression in primary s.c. tumors induced by the indicated cell lines. Shown are protein expression data from 2 representative mice injected with the indicated control, N-cadherin and cadherin-11 transfectants. Bar = 100 μm.

presence of calcium ions. Nevertheless, since we observed binding of exogenous cadherins to endogenous β-catenin, together with their cell-surface localization, these data strongly suggest that the exogenous cadherin molecules are functional.

LM8 subclones overexpressing N-cadherin and cadherin-11 showed significant inhibition in cell motility in the *in vitro* migration assay system. Unfortunately, we were not able to determine whether there were any differences in invasive ability using, *e.g.,* Matrigel invasion assays or extracellular matrix–coated filters, because Dunn and LM8 cells express very low levels of matrix metalloproteinase (MMP)-9/gelatinase B[27] and cannot penetrate efficiently through such matrices (data not shown; Dr. K. Itoh, Osaka Medical Center, Japan, personal communication). Nevertheless, the suppressed cell migration ability in N-cadherin and cadherin-11 transfectants was an initial indication that overexpression of these cadherins altered a key cellular function which could be involved in their ability to metastasize. Indeed, our *in vivo* studies clearly demonstrated that N-cadherin- and cadherin-11-overexpressing LM8 cells were significantly impaired in their ability to form pulmonary metastasis compared to control transfectants. This was supported by several parameters, including a decrease in not only the number of metastases but also the weight of the lungs. One cadherin-11-overexpressing clone, LM8-OB8, did not show a significant reduction in the number of lung metastases, and this was likely due to low levels of exogenous cadherin-11. However, the reduced size of lung foci and decreased lung weight following injection of OB8 cells confirmed the functionality of this cadherin.

The mechanisms responsible for the reduced metastatic potential of the cadherin clones are not clear. One possibility is that high levels of these cadherins in osteosarcoma cells may enhance cell–cell clustering and adhesion during the growth and development of primary tumors and prevent them from entering into the circulation. Another possibility is that altered levels of proteases such as MMPs, MT-MMPs and urokinase, following cadherin overexpression may contribute to the reduced metastatic ability.[32] Finally, it is possible that high expression of exogenous cadherins may alter the expression of Rho-family GTPases and the cytoskeleton, which have been implicated in tumor metastasis.[32]

In addition to the decreased number of lung metastases, we observed a significant reduction in the size and weight of primary s.c. tumors between N-cadherin- and cadherin-11-overexpressing clones and control transfectants. Thus, it is possible that cadherin overexpression caused inhibition in cell growth, as has been observed in E-cadherin-overexpressing epithelial cells *in vitro.*[33] However, our *in vitro* observations that N-cadherin- and cadherin-11-overexpressing clones did not exhibit any altered proliferation rates suggest that the reduced metastatic activity is not due to reduced cell proliferation, although we have not assessed this *in vivo.* Moreover, it is also not yet clear whether the reduced tumor size is a cell-autonomous effect: since normal fibroblasts express N-cadherin and cadherin-11, it is possible that there are some interactions between the injected tumor cells and the host connective tissue cells which could lead to altered tumor growth, *e.g.,* expression of *Vegf-D,* which is known to be upregulated by cadherin-11.[34] Thus, in osteosarcoma, it would be interesting to investigate further not only the behavior of the tumor cells but also the responsiveness of the normal bone environment, including reactive bone formation and resorption. This can be done *via* orthotopic inoculation, whereby cadherin-overexpressing LM8 cells are inoculated directly into the bone marrow space, as has been demonstrated previously.[35]

Our observation that overexpression of N-cadherin and cadherin-11 in osteosarcoma cells inhibits their *in vivo* metastatic potential is in apparent contrast to reports that highly invasive breast or prostate cancer cell lines express cadherin-11 or N-cadherin[30,36,37] and that introduction of these cadherins into breast cancer or melanoma cell lines promotes *in vitro* cell motility and invasion and further *in vivo* metastasis.[38,39] These differences might reflect differences between carcinomas and sarcomas, which originate from epithelial cells and stromal cells, respectively, and suggest that the cellular context must be taken into consideration. Indeed, cadherins are expressed in a tissue-specific manner,[6] implying that they have specific functions in these tissues as well as in different types of tumor. Osteoblasts express high levels of N-cadherin and cadherin-11, which are important for cell–cell interaction.[16–21,25] In our previous study, expression of N-cadherin and cadherin-11 was suppressed in human osteosarcoma, which is characterized by not only irregular bone formation but also ag-

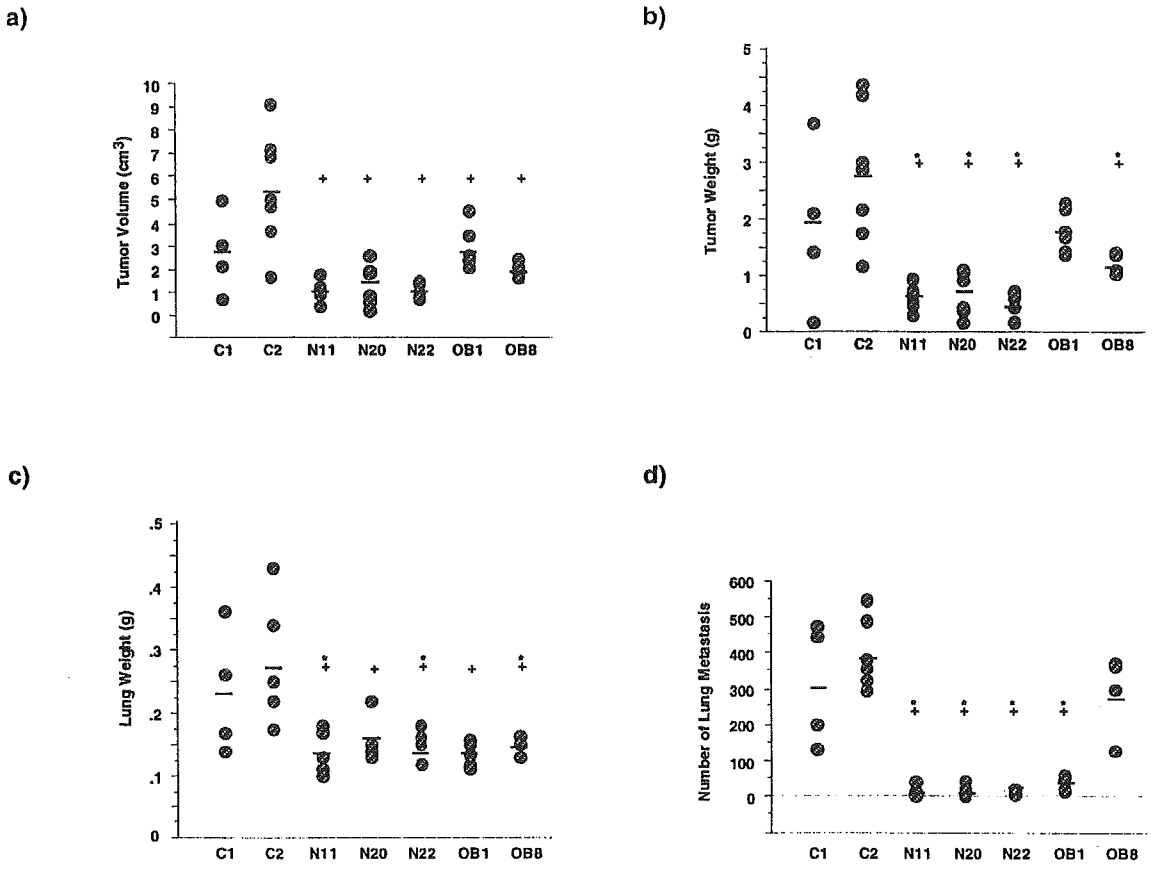

FIGURE 5 – Quantification of primary and metastatic lesions induced by cadherin transfectants *in vivo*. Volume *(a)* and weight *(b)* of primary s.c. tumors were quantified, as well as total weight of lungs *(c)* and number of lung metastases *(d)*. Raw data (hatched circles) and means (black bars) are indicated for each cell clone. Data were analyzed by Dunnett's *post-hoc* test. * and + indicate statistical significance ($p < 0.05$) compared to C1 and C2, respectively.

gressive invasion and lung metastasis. An example of tissue specificity is shown by the report that downregulation of cadherin-11 occurs in astrocytoma, whereas normal brain tissue expresses both N-cadherin and cadherin-11.[40] In contrast, E-cadherin is highly expressed in normal epithelial cells or in epidermal melanocytes, to maintain tissue structure.[38,39] Thus, introducing N-cadherin or cadherin-11 into carcinoma or melanoma cell lines might have different consequences compared to introducing them into osteosarcoma cells. Moreover, the so-called epithelial-to-mesenchymal transition has been suggested to be important for invasion of carcinoma,[41] which includes a cadherin class switch from E-cadherin to N-cadherin or cadherin-11,[42,43] further supporting the notion that N-cadherin and cadherin-11 play distinct roles in epithelial and mesenchymal tissues.

Although the function of N-cadherin in tumor cell invasion has been reported *in vitro*, the *in vivo* data remain controversial. The only study that has directly addressed the role of E-cadherin *in vivo* showed that transgenic expression of a dominant-negative E-cadherin driven by an insulin promoter increases the transformation from adenoma to carcinoma of pancreatic β-cell tumors in transgenic mice.[44] In the transition from adenoma to carcinoma, expression of E-cadherin is lost but N-cadherin is still expressed. Since such a dominant-negative cadherin lacking an extracellular domain would interfere with all cadherin molecules,[45] it is likely that the function of N-cadherin is also blocked in the carcinomas of double-transgenic mice, which developed organ metastasis. Taken together, these data are consistent with the possibility that N-cadherin plays an important functional role in preventing metastasis *in vivo*.

In conclusion, we have shown that reduced expression of N-cadherin and cadherin-11 in murine osteosarcoma cells is a requirement for the formation of lung metastases. This is consistent with our previous demonstration that altered expression of these cadherins is associated with human osteosarcomas and metastasis. Interestingly, we have performed preliminary experiments using transgenic mice overexpressing the c-*fos* protooncogene, which develop osteosarcomas[46,47] but do not form any lung metastases, and have shown that these tumors express both N-cadherin and cadherin-11.[48] Since it is well established that loss of E-cadherin function is important for carcinoma progression and metastasis,[10,11] it may be that dysfunction of N-cadherin and cadherin-11 plays a similar role in osteosarcoma. Studies in which cadherin expression during c-Fos-induced osteosarcoma formation is downregulated are currently under way and will provide further functional evidence that these cadherins are key regulators of osteosarcoma progression and metastasis.

ACKNOWLEDGEMENTS

The authors thank Dr. K. Itoh for helpful advice, Dr. I. Kii for providing L-cell transfectants and Dr. A. Yeudall for critical reading of the manuscript. T.K. was supported by a fellowship from the Canon Europe Foundation.

REFERENCES

1. Schajowicz F. WHO: Histological typing of bone tumors, 2nd ed. Berlin: Springer-Verlag, 1993. 10–13.
2. Wunder JS, Bull SB, Aneliunas V, Lee PD, Davis AM, Beauchamp CP, Conrad EU, Grimer RJ, Healey JH, Rock MJ, Bell RS, Andrulis IL. *MDR1* gene expression and outcome in osteosarcoma: a prospective, multicenter study. J Clin Oncol 2000;18:2685–94.
3. Whelan JS. Osteosarcoma. Eur J Cancer 1997;33:1611–8.
4. Hanahan D, Weinberg RA. The hallmarks of cancer. Cell 2000;100: 57–70.
5. Kim J, Yu W, Kovalski K, Ossowski L. Requirement for specific proteases in cancer cell intravasation as revealed by a novel semiquantitative PCR-based assay. Cell 1998;94:353–62.
6. Takeichi M. Cadherin cell adhesion receptors as a morphogenetic regulator. Science 1991;251:1451–5.
7. Angst BD, Marcozzi C, Magee AI. The cadherin superfamily: diversity in form and function. J Cell Sci 2001;114:629–41.
8. Provost E, Rimm DL. Controversies at the cytoplasmic face of the cadherin-based adhesion complex. Curr Opin Cell Biol 1999;11:567–72.
9. Nagafuchi A. Molecular architecture of adherens junctions. Curr Opin Cell Biol 2001;13:600–3.
10. Christofori G, Semb H. The role of the cell-adhesion molecule E-cadherin as a tumour-suppressor gene. Trends Biochem Sci 1999;24: 73–6.
11. Hirohashi S. Inactivation of the E-cadherin-mediated cell adhesion system in human cancers. Am J Pathol 1998;153:333–9.
12. Kawanishi J, Kato J, Sasaki K, Fujii S, Watanabe N, Niitsu Y. Loss of E-cadherin-dependent cell–cell adhesion due to mutation of the beta-catenin gene in a human cancer cell line, HSC-39. Mol Cell Biol 1995;15:1175–81.
13. Aono S, Nakagawa S, Reynolds AB, Takeichi M. p120(ctn) acts as an inhibitory regulator of cadherin function in colon carcinoma cells. J Cell Biol 1999;145:551–62.
14. Behrens J. Control of beta-catenin signaling in tumor development. Ann NY Acad Sci 2000;910:21–33.
15. Manolagas SC. Birth and death of bone cells: basic regulatory mechanisms and implications for the pathogenesis and treatment of osteoporosis. Endocr Rev 2000;21:11537.
16. Bennett JH, Moffatt S, Horton M. Cell adhesion molecules in human osteoblasts: structure and function. Histol Histopathol 2001;16:603–11.
17. Kawaguchi J, Takeshita S, Kashima T, Imai T, Machinami R, Kudo A. Expression and function of the splice variant of the human cadherin-11 gene in subordination to intact cadherin-11. J Bone Miner Res 1999;14:764–75.
18. Kawaguchi J, Kii I, Sugiyama Y, Takeshita S, Kudo A. The transition of cadherin expression in osteoblast differentiation from mesenchymal cells: consistent expression of cadherin-11 in osteoblast lineage. J Bone Miner Res 2001;16:260–9.
19. Ferrari SL, Traianedes K, Thorne M, Lafage-Proust MH, Genever P, Cecchini MG, et al. A role for N-cadherin in the development of the differentiated osteoblastic phenotype. J Bone Miner Res 2000;15: 198–208.
20. Cheng SL, Shin CS, Towler DA, Civitelli R. A dominant negative cadherin inhibits osteoblast differentiation. J Bone Miner Res 2000; 15:2362–70.
21. Marie PJ. Role of N-cadherin in bone formation. J Cell Physiol 2002;190:297–305.
22. Okazaki M, Takeshita S, Kawai S, Kikuno R, Tsujimura A, Kudo A, et al. Molecular cloning and characterization of OB-cadherin, a new member of cadherin family expressed in osteoblasts. J Biol Chem 1994;269:12092–8.
23. Hoffmann I, Balling R. Cloning and expression analysis of a novel mesodermally expressed cadherin. Dev Biol 1995;169:337–46.
24. Kimura Y, Matsunami H, Inoue T, Shimamura K, Uchida N, Ueno T, et al. Cadherin-11 expressed in association with mesenchymal morphogenesis in the head, somite, and limb bud of early mouse embryos. Dev Biol 1995;169:347–58.
25. Kawaguchi J, Azuma Y, Hoshi K, Kii I, Takeshita S, Ohta T, et al. Targeted disruption of cadherin-11 leads to a reduction in bone density in calvaria and long bone metaphyses. J Bone Miner Res 2001;16:1265–71.
26. Kashima T, Kawaguchi J, Takeshita S, Kuroda M, Takanashi M, Horiuchi H, et al. Anomalous cadherin expression in osteosarcoma. Possible relationships to metastasis and morphogenesis. Am J Pathol 1999;155:1549–55.
27. Asai T, Ueda T, Itoh K, Yoshioka K, Aoki Y, Mori S, et al. Establishment and characterization of a murine osteosarcoma cell line (LM8) with high metastatic potential to the lung. Int J Cancer 1998; 76:418–22.
28. Hippo Y, Yashiro M, Ishii M, Taniguchi H, Tsutsumi S, Hirakawa K, et al. Differential gene expression profiles of scirrhous gastric cancer cells with high metastatic potential to peritoneum or lymph nodes. Cancer Res 2001;61:889–95.
29. Niwa H, Yamamura K, Miyazaki J. Efficient selection for high-expression transfectants with a novel eukaryotic vector. Gene 1991; 108:193–9.
30. Nieman MT, Prudoff RS, Johnson KR, Wheelock MJ. N-Cadherin promotes motility in human breast cancer cells regardless of their E-cadherin expression. J Cell Biol 1999;147:631–44.
31. Shimoyama Y, Hirohashi S, Hirano S, Noguchi M, Shimosato Y, Takeichi M, et al. Cadherin cell-adhesion molecules in human epithelial tissues and carcinomas. Cancer Res 1989;49:2128–33.
32. Fukata M, Kaibuchi K. Rho-family GTPases in cadherin-mediated cell–cell adhesion. Nat Rev Mol Cell Biol 2001;2:887–97.
33. Stockinger A, Eger A, Wolf J, Beug H, Foisner R. E-Cadherin regulates cell growth by modulating proliferation-dependent beta-catenin transcriptional activity. J Cell Biol 2001;154:1185–96.
34. Orlandini M, Oliviero S. In fibroblasts Vegf-D expression is induced by cell–cell contact mediated by cadherin-11. J Biol Chem 2001;276: 6576–81.
35. Khanna C, Khan J, Nguyen P, Prehn J, Caylor J, Yeung C, et al. Metastasis-associated differences in gene expression in a murine model of osteosarcoma. Cancer Res 2001;61:3750–9.
36. Tran NL, Nagle RB, Cress AE, Heimark RL. N-Cadherin expression in human prostate carcinoma cell lines. An epithelial–mesenchymal transformation mediating adhesion with stromal cells. Am J Pathol 1999;155:787–98.
37. Pishvaian MJ, Feltes CM, Thompson P, Bussemakers MJ, Schalken JA, Byers SW. Cadherin-11 is expressed in invasive breast cancer cell lines. Cancer Res 1999;59:947–52.
38. Li G, Satyamoorthy K, Herlyn M. N-Cadherin-mediated intercellular interactions promote survival and migration of melanoma cells. Cancer Res 2001;61:3819–25.
39. Hazan RB, Phillips GR, Qiao RF, Norton L, Aaronson SA. Exogenous expression of N-cadherin in breast cancer cells induces cell migration, invasion, and metastasis. J Cell Biol 2000;148:779–90.
40. Zhou R, Skalli O. Identification of cadherin-11 down-regulation as a common response of astrocytoma cells to transforming growth factor-alpha. Differentiation 2000;66:165–72.
41. Thiery JP. Epithelial–mesenchymal transitions in tumour progression. Nat Rev Cancer 2002;2:442–54
42. Shibata T, Ochiai A, Gotoh M, Machinami R, Hirohashi S. Simultaneous expression of cadherin-11 in signet-ring cell carcinoma and stromal cells of diffuse-type gastric cancer. Cancer Lett 1996;99:147–53.
43. Tomita K, van Bokhoven A, van Leenders GJ, Ruijter ET, Jansen CF, Bussemakers MJ, et al. Cadherin switching in human prostate cancer progression. Cancer Res 2000;60:3650–4.
44. Perl AK, Wilgenbus P, Dahl U, Semb H, Christofori G. A causal role for E-cadherin in the transition from adenoma to carcinoma. Nature 1998;392:190–3.
45. Dahl U, Sjodin A, Semb H. Cadherins regulate aggregation of pancreatic beta-cells in vivo. Development 1996;122:2895–902.
46. Grigoriadis AE, Schellander K, Wang ZQ, Wagner EF. Osteoblasts are target cells for transformation in c-fos transgenic mice. J Cell Biol 1993;122:685–701.
47. Wang ZQ, Liang J, Schellander K, Wagner EF, Grigoriadis AE. c-fos-induced osteosarcoma formation in transgenic mice: cooperativity with c-jun and the role of endogenous c-fos. Cancer Res 1995; 55:6244–51.
48. Kashima T, Nakamura K, Kawaguchi K, Kudo A, Grigoriadis AE. A possible functional role of cadherins to prevent osteosarcoma metastasis. J Bone Miner Res 2002;17(Suppl):S408.

Int. J. Cancer: **103,** 455–465 (2003)

Publication of the International Union Against Cancer

GLYPICAN-3, OVEREXPRESSED IN HEPATOCELLULAR CARCINOMA, MODULATES FGF2 AND BMP-7 SIGNALING

Yutaka MIDORIKAWA[1,2], Shumpei ISHIKAWA[1], Hiroko IWANARI[3], Takeshi IMAMURA[4], Hirohiko SAKAMOTO[5], Kohei MIYAZONO[4], Tatsuhiko KODAMA[6], Masatoshi MAKUUCHI[2], and Hiroyuki ABURATANI[1]*

[1]*Genome Science Division, Research Center for Advanced Science and Technology, University of Tokyo, Tokyo, Japan*
[2]*Hepato-Biliary-Pancreatic Surgery Division, Department of Surgery, University of Tokyo, Tokyo, Japan*
[3]*Institute of Immunology, Tokyo, Japan*
[4]*Department of Biochemistry, The Cancer Institute, Tokyo, Japan*
[5]*Department of Surgery, Saitama Cancer Center, Tokyo, Japan*
[6]*Molecular Biology and Medicine, Research Center for Advanced Science and Technology, University of Tokyo, Tokyo, Japan*

The Glypican (GPC) family is a prototypical member of the cell-surface heparan sulfate proteoglycans (HSPGs). The HSPGs have been demonstrated to interact with growth factors, act as coreceptors and modulate growth factor activity. Here we show that based on oligonucleotide array analysis, GPC3 was upregulated in hepatocellular carcinoma (HCC). By northern blot analysis, GPC3 mRNA was found to be upregulated in 29 of 52 cases of HCC (55.7%). By Western blot analysis carried out with a monoclonal anti-GPC3 antibody we generated, the GPC3 protein was found to be overexpressed in 6 hepatoma cell lines, HepG2, Hep3B, HT17, HuH6, HuH7 and PLC/PRF/5, as well as 22 tumors (42.3%). To investigate the role of overexpressed GPC3 in liver cancer, we analyzed its effects on cell growth of hepatoblastoma-derived cells. Overexpression of GPC3 modulated cell proliferation by inhibiting fibroblast growth factor 2 (FGF2) and bone morphogenetic protein 7 (BMP-7) activity. An interaction of GPC3 and FGF2 was revealed by co-immunoprecipitation, while GPC3 was found to inhibit BMP-7 signaling through the Smad pathway by reporter gene assay. The modulation of growth factors by GPC3 may help explain its role in liver carcinogenesis. In addition, the ability of HCC cells to express GPC3 at high levels may serve as a new tumor marker for HCC.

Key words: *heparan sulfate proteoglycan; hepatocarcinogenesis; heparin-binding growth factors; tumor marker; cell proliferation*

Glypican 3 (GPC3) is a member of the heparan sulfate proteoglycans (HSPGs) and binds to the cell membrane via glycosilphosphatidylinositol anchors.[1] HSPGs are well known to interact with growth factors through heparan sulfate (HS) chains, to act as a coreceptor for heparin binding growth factors and ultimately, to stimulate or inhibit growth factor activity.[2–4] HSPGs have been recently identified to act as coreceptors for fibroblast growth factor 2 (FGF2), to promote it to bind its receptor and finally, to play an important role in the FGF2 signaling pathway.[5–9]

On the other hand, bone morphogenetic protein (BMP), a secreted growth factor and a subset of transforming growth factor-β (TGF-β) superfamily, regulates cell proliferation and apoptosis during morphogenesis of bone, renal and neuronal tissues.[3] Among the BMP family members, BMP-7 is known to control collecting tubule cell proliferation and apoptosis in a dose-dependent manner[10] and GPC3 is reported to modulate BMP-mediated effects during renal branching morphogenesis using GPC3-/mouse.[4]

Clinically, it has been reported that the GPC3 gene is mutated in Simpson-Golabi-Behmel syndrome, an X-linked disorder characterized by pre- and postnatal overgrowth.[11] GPC3 is also reported to be able to interact with insulin-like growth factor 2 (IGF2), mediated by the HS chains and an altered regulation of IGF2,[11] although the binding of GPC3 to IGF2 is still controversial.[12] Such evidence suggest that GPC3 could well be involved in the control of cell proliferation and/or the induction of apoptosis, as indicated by certain experimental studies.[13,14]

In cancer tissues, the levels of transcriptionally expressed GPC3 are variable, although overexpression of the protein has yet to be conclusively demonstrated. In ovarian cancer, it is reported that GPC3 is expressed in the normal ovary, but that silencing of this gene takes place in a significant proportion of ovarian cancer cell lines as a result of hypermethylation of the GPC3 promoter. Therefore, GPC3 has come to be understood to be a suppressor gene in the ovary.[14] Downregulation of GPC3 in mesothelioma indeed has been reported, whereas GPC3 is highly expressed in normal mesothelial cells.[15] Accordingly, the function of GPC3 in the ovary, like that in the mesothelium, is thought to either induce apoptosis or control cell proliferation.

In contrast, GPC3 mRNA has also been demonstrated to be highly expressed in embryonal tumors,[16] colon cancer[17] and hepatocellular carcinoma (HCC)[18,19] in comparison with the corresponding normal tissues. However, an upregulation of GPC3 in cancerous tissues is contradictory to the commonly understood function of this molecule and, therefore, the function of GPC3 has been hypothesized to be varied in a tissue-specific manner, that is, GPC3 induces apoptosis in breast or ovary, but acts as oncofetal protein in liver and colon.[13]

In our study, it was found that the GPC3 mRNA is highly expressed in HCC, as shown by gene expression profile analysis and validated by Northern blot. To confirm overexpression of GPC3 protein, we generated a monoclonal anti-GPC3 antibody and performed immunohistochemistry and Western blot analysis. To determine the role of GPC3 in hepatocarcinogenesis, we established a liver cancer cell line, in which GPC3 expression can be induced by tetracycline withdrawal. We show here that GPC3 interacts with FGF2, inhibits the BMP-7 signaling pathway and modulates the activity of FGF2 and BMP-7. All of these findings suggest that GPC3 does not only regulate cell proliferation under certain conditions but that it also plays an important role in hepatocarcinogenesis.

Grant sponsor: The Ministry of Education, Science, Sports and Culture of Japan (H.A.). Grant numbers: Grants-in-Aid for Scientific Research (B) 12557051 and 13218019 and Scientific Research on Priority Areas (C) 12217031. Grant sponsor: Uehara Memorial Foundation; Grant sponsor: Sagawa Foundation for Promotion of Cancer Research.

*Correspondence to: Genome Science Division, Research Center for Advanced Science and Technology, The University of Tokyo, 4-6-1 Komaba, Meguro-ku, Tokyo 153-8904, Japan. Fax: +81-3-5452-5355. E-mail: haburata-tky@umin.ac.jp

Received 2 April 2002; Revised 12 August 2002; Accepted 21 September 2002

DOI 10.1002/ijc.10856

MATERIAL AND METHODS

Tissue samples

Forty-five patients with HCC who had undergone hepatectomy at either the Hepato-Biliary-Pancreatic Surgery Division, Department of Surgery, Graduate School of Medicine, University of Tokyo, or at the Department of Surgery, Saitama Cancer Center, were included in our study after obtaining informed consent. According to the definition of multicentric HCCs proposed by Tsuda *et al.*,[20] 5 patients were diagnosed as having 2 multicentric nodules and 1 patient 3 nodules; therefore, 52 tumors and 45 noncancerous liver tissues were taken. As controls, normal liver tissues were obtained from 8 patients with metastatic liver cancer. The average of 45 patients including 30 male and 15 female was 64.4 ± 7.7 years. Serum test showed 11 patients were positive for hepatitis B surface antigen and 34 for hepatitis C virus antibody. Histologic findings demonstrated that of 52 tumors, 22 were well-differentiated hepatocellular carcinoma (WD), 21 moderately differentiated hepatocellular carcinoma (MD) and 9 poorly differentiated hepatocellular carcinoma (PD), whereas the background liver of 13 patients were chronic hepatitis (CH) and 32 liver cirrhosis (LC).

Six tumors were accompanied with vascular invasion and the average of tumor size was 28.0 ± 13.7 mm in diameter. The surgical specimens were immediately cut into small pieces after resection, snap-frozen in liquid nitrogen and stored in a −80°C freezer.

Cell lines and culture conditions

The hepatoblastoma cell line HepG2 was obtained from the American Type Culture Collection. HCC cell lines Hep3B, HT17 and Li-7 were kindly provided by Cell Resource Center for Biomedical Research, Tohoku University (Miyagi, Japan). The HCC cell lines HLE, HuH7 and PLC/PRF/5 and the hepatoblastoma cell line HuH6 were purchased from Health Science Research Resource Bank (Osaka, Japan). HepG2, Hep3B, HLE, HuH6 and PLC/PRF/5 were maintained in DMEM (Sigma, St Louis, MO), HT17 was maintained in MEM (Sigma) and HuH7 and Li7 in RPMI 1640 (Sigma). Tetracycline-regulated HepG2 cells (HY-Toff) were a gift from Dr. Ying Huang (University of Tokyo).[21]

Vector construction and transfection

cDNA synthesized from colon cancer cell line, Caco2, which has no abnormality of GPC3 sequence, was used as a template for RT-PCR using Advantage II (Clontech, Palo Alto, CA). After confirmation of GPC3 coding with an API Prism 3100 Genetic Analyzer (Applied Biosystems, Foster City, CA), GPC3 cDNA

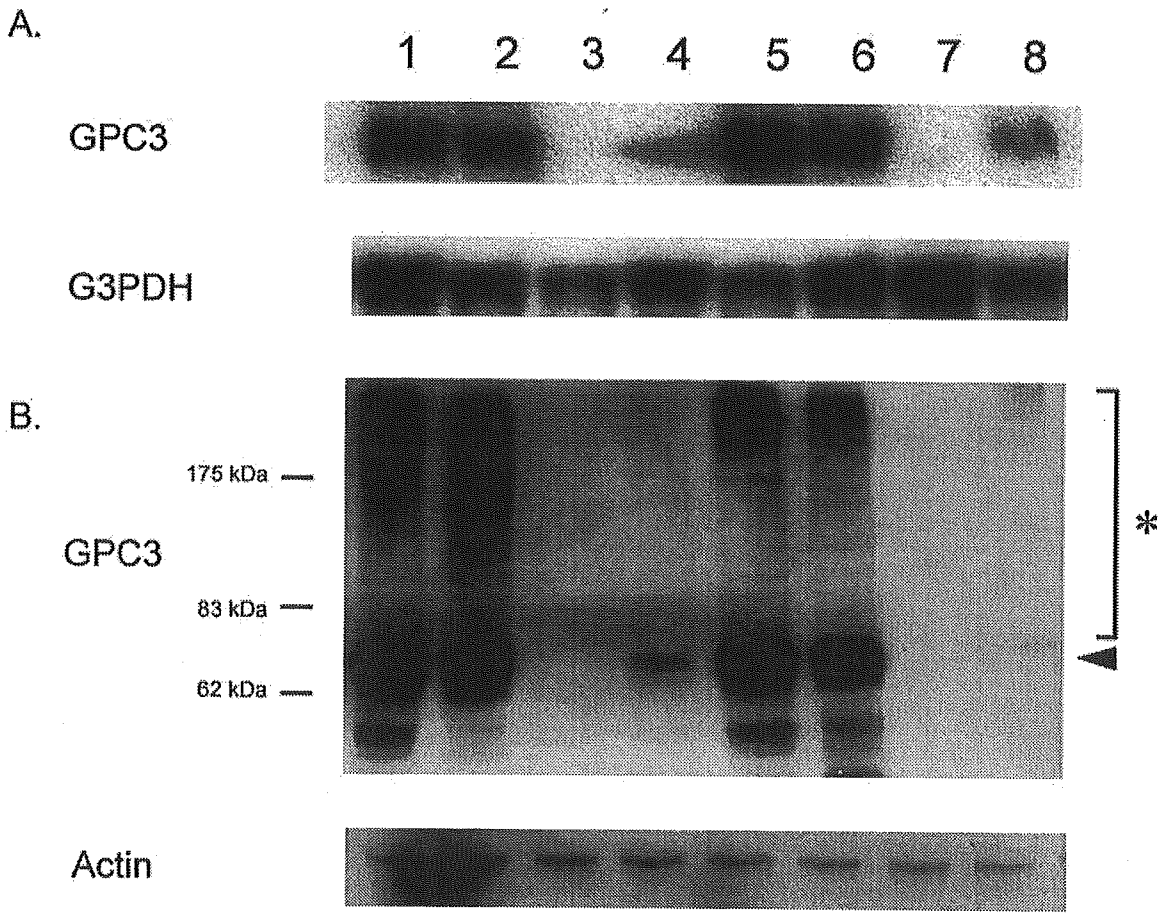

FIGURE 1 – Expression of GPC3 mRNA and protein in hepatoma cell lines. *(a)* Northern blot analysis of the GPC3 expression levels in hepatoma cell lines. Lane 1, HepG2; lane 2, Hep3B; lane 3, HLE; lane 4, HT17; lane 5, HuH6; lane 6, HuH7; lane 7, Li-7; lane 8, PLC/PRF/5. *(b)* Western blot analysis of the GPC3 expression levels in hepatoma cell lines. Arrowhead, core protein of GPC3; asterisk, glycosylated protein. Numbers on the left represent molecular mass markers.

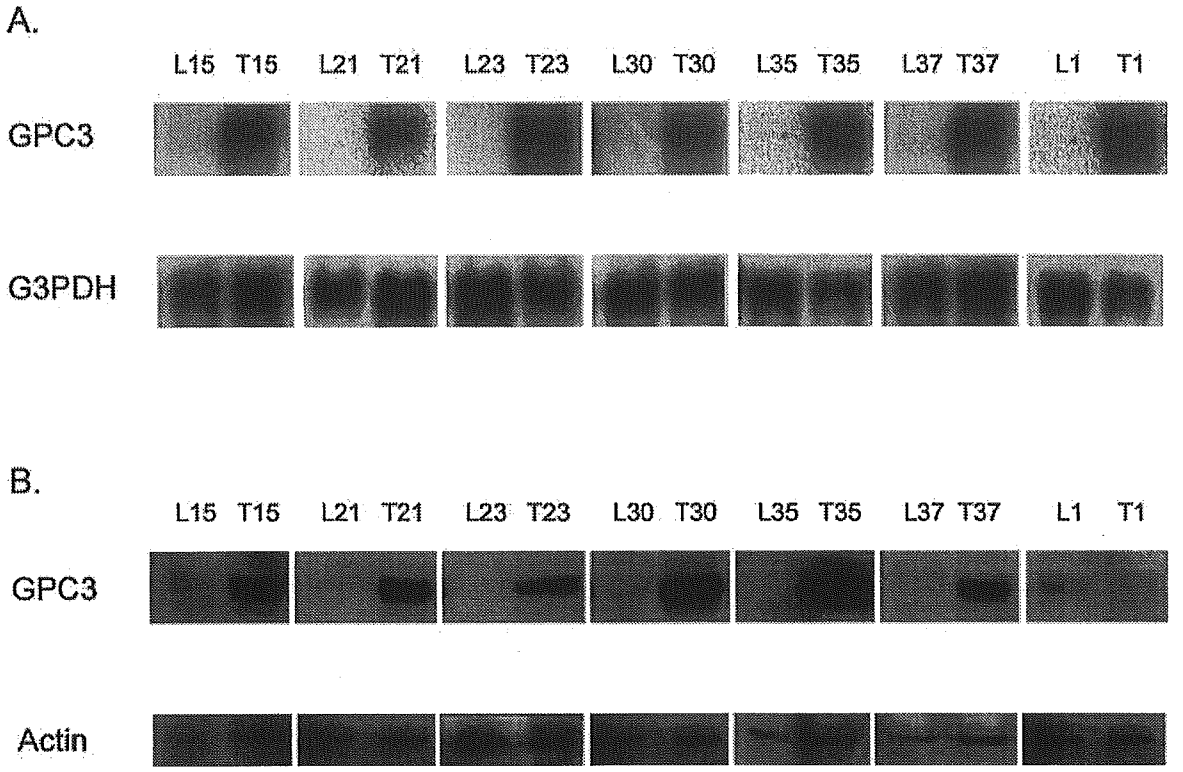

FIGURE 2 – Expression of GCP3 in hepatocellular carcinoma and noncancerous tissues. *(a)* Northern blot analysis of the GPC3 expression levels in paired noncancerous tissues (L) and HCC (T). The number on the top of the figure refers to the patient's no., shown in Table I. *(b)* Western blot analysis of the GPC3 expression levels of paired noncancerous tissues (L) and HCC (T).

was subcloned into the pBI-EGFP vector (Clontech) and termed pBI-EGFP-GPC3. The primers used for the GPC3 preparation contained an *Eco*RV and *Nhe*I site, respectively, attached to the 5′ end, a sense primer, 5′-GATATC-ATGGCCGGGACCGTGCG-CACCGCGT and an antisense primer, 5′-GCTAGC-TCAGTG-CACCAGGAAGAAGAAGCAC. To generate a HY-Toff cell line with tetracycline-inducible GPC3 expression, HY-Toff cells were cotransfected with both pBI-EGFP-GPC3 and pBabepuro using a Tfx-20 (Promega, Madison, WI), followed by selection in culture medium containing 2 μg/ml puromycin (Nacalai tesque, Kyoto, Japan) and 5 ng/ml Doxycycline hydrochloride (Dox) (Sigma). Surviving clones were isolated, expanded and dubbed HY-Toff-GPC3 clones. To induce GPC3 expression, cells were incubated without Dox in serum-containing medium.

RNA extraction and Northern blot analysis

Total RNA was isolated from frozen tissue with an ISOGENE™ kit (Nippon Gene, Tokyo, Japan), according to the manufacturer's protocol. The Northern blot analysis, using 10 μg total RNA, was performed as described.[22] ^{32}P-radiolabeled cDNA probes were prepared with a Strip-EZ DNA kit (Ambion, Austin, TX) using a human GPC3 cDNA as templates.

Generation of monoclonal antibody against GPC3

A peptide composed of 17 amino acid residues, from 355 to 371 of GPC3, was chemically synthesized (Peptide Institute, Osaka, Japan). Female BALB/c mice (6 weeks of age) were immunized 3 times every 2 weeks with the synthetic peptide GPC3 conjugated with the Keyhole Lmpet Hemocyanin (KLH; Calbiochem, San Diego, CA). Spleen cells were isolated 3 days after the last immunization and fused with NS-1 myeloma cells (Dainippon Pharmaceutical, Osaka, Japan) by a conventional method.[23] Hybridomas were selected by the enzyme-linked immunosorbent assay (ELISA) with the synthetic peptide in each well of a 96-well titer plate (Corning, Acton, MA). Peroxidase-conjugated anti-mouse IgG antibody (ICN Pharmaceuticals, Costa Mesa, OH) was used as the second antibody. Absorbence at 450 nm was measured following incubation with TMB Soluble Reagent (ScyTek, Logan, UT). Positive hybridomas were cloned by limited dilution. The large-scale production of monoclonal antibodies was carried out by growing the hybridoma cells in mouse ascites. The immunoglobulin was purified by ammonium sulfate precipitation.

Protein extraction, Western blot and immunohistochemical analysis

Cells and tissue samples were lysed in a lysis buffer [20mM HEPES (pH 7.5), 150 mM NaCl, 1 mM EDTA, 10 μg/ml, 1 mM PMSF, 1.0% Triton X-100, 0.5% deoxycholate, 0.1% SDS] after collection from a 100 mm dish and disruption, respectively. Proteins (20 μg) were resolved on 7.5% SDS-PAGE and transferred to Hybond-P membranes (Amersham Pharmacia, Piscataway, NJ). Western blot analysis was performed using anti-GPC3 antibody, with anti-actin (Santa Cruz, Santa Cruz, CA) as control. After incubation with horseradish peroxidase-conjugated antibody sheep anti-mouse IgG (Amersham Pharmacia), labeled proteins were detected with an ECL-Plus detection system (Amersham Pharmacia).

For the detection of GPC3 on the cell surface of HCC cells, noncancerous and cancerous tissues with or without GPC3 expression as determined by Western blot analysis were subjected to

TABLE I – CLINICAL DATA AND PATHOLOGIC FINDINGS ACCORDING TO GPC3 EXPRESSION

Patient no.	Age	Gender	HVI	BGL	Diff. grade	VI	Tumor Size (mm)	NB (HCC)	NB (Liver)	WB (HCC)	WB (Liver)
1	48	M	HB	LC	WD	–	22	++	–	–	+
2	69	M	HC	LC	WD	–	15	+	–	–	–
3	72	F	HC	CH	WD	–	33	–	–	–	–
4	69	F	HC	LC	WD	–	40	–	–	–	–
5	62	M	HB	CH	WD	–	31	–	–	–	–
6	64	M	HC	LC	WD	–	15	–	–	–	–
7	59	F	HC	LC	WD	–	20	–	–	–	–
8	70	M	HC	LC	WD	–	16	–	–	–	–
9	75	M	HC	CH	WD	–	40	–	–	–	–
10	67	M	HC	LC	WD	–	17	–	–	–	–
11	62	M	HC	CH	WD	–	25	–	–	–	–
12	66	M	HC	CH	WD	+	36	–	–	–	–
13	67	M	HC	LC	WD	–	26	–	–	–	–
14	68	M	HC	LC	WD	–	22	–	–	–	–
15	66	M	HC	LC	WD	–	23	+++	–	++	–
16	62	F	HC	LC	WD	–	15	+	–	–	–
17	71	M	HB	LC	WD	–	22	+	–	+	–
18	65	M	HC	LC	MD	–	21	–	–	–	+
19	69	F	HB	LC	MD	–	38	–	–	–	–
20	60	M	HC	LC	MD	–	65	–	–	+	+
21	47	M	HB	CH	MD	+	24	+++	–	++	–
22	71	F	HC	LC	MD	–	22	++	–	++	–
23	71	F	HC	LC	MD	–	30	+++	–	+++	–
24	69	M	HC	CH	MD	–	50	–	–	–	–
25	70	F	HC	LC	MD	–	23	+++	–	+++	–
26	53	M	HB	LC	MD	–	45	–	–	–	–
27	63	F	HC	CH	MD	–	20	+++	–	+++	–
28	50	M	HB	LC	MD	+	25	++	–	+	+
29	49	M	HB	LC	MD	+	22	++	–	+++	–
30	61	F	HC	LC	MD	–	41	+++	+	++	–
31	48	M	HB	LC	MD	–	35	+	–	–	–
32	78	M	HC	LC	PD	–	43	–	–	–	–
33	54	M	HB	CH	PD	–	11	++	–	+	+
34	68	F	HC	CH	PD	–	23	–	–	–	–
35	56	F	HB	CH	PD	–	42	+++	–	+++	–
36	73	F	HC	LC	PD	–	24	–	+	–	–
37	70	F	HC	LC	PD	+	30	+++	–	++	–
38	63	M	HC	LC	PD	–	35	++	+	++	–
39	72	M	HC	CH	PD	–	89	++	–	+++	–
40	71	M	HC	LC	WD	–	13	–	–	–	–
					MD	–	15	+++		++	
41	63	M	HC	LC	WD	–	20	+	–	–	–
					MD	–	20	++		–	
42	66	F	HC	LC	WD	–	40	++	–	+	–
					MD	–	27	++		++	
43	70	M	HC	LC	WD	–	13	+	–	–	–
					PD	+	22	++		++	
44	70	M	HC	LC	MD	–	25	–	–	–	–
					MD	–	20	++		+	
45	65	M	HC	CH	WD	–	20	++	+	–	–
					MD	–	25	+		–	
					MD	–	22	–		–	

HVI, hepatitis viral infection; BGL, background liver; VI, vascular invasion; NB, Northern blot analysis; WB, Western blot analysis; M, male; F, female. –, GPC3 negative; +, weakly positive; ++, moderately positive; +++, strongly positive in NB and WB. Patient nos. 1–39 have 1 tumor; nos. 40–44, 2 tumors; no. 45 3 tumors.

immunohistochemistry using an LSAB system. After 5 μm-thick frozen sections on glass slides were fixed by ethanol and treated using proteinase K, sections were stained with anti-GPC3 antibody by means of an LSAB kit/HRP (Dako, Glostrup, Denmark A/S) according to the manufacturer's protocol.

Cell growth assay

Cell growth assay was performed in the same manner as described previously.[24] Briefly, 3 independent HY-Toff-GPC3 clones were plated overnight at a density of 10,000 cells/well in 96-well plates, washed with PBS and subsequently incubated in 100 μl DMEM with 1% FBS in the presence or absence of Dox in order to control GPC3 expression. Growth factors, IGF2, FGF2, BMP-7, TGF-β3 or HB-EGF (R&D Systems, Minneapolis, MN), were added at various concentrations. Forty-eight hours after incubation, cells were counted with an MTT Cell Growth Kit (Chemicon International, Temecula, CA) and compared in triplicate in each clone.

Purification of FGF2 and GPC3 protein complex

Human FGF2 coding cDNA was obtained by the same method described above, using the sense primer, 5′-GAATTC-ATGGC AGCCGGGAGCATCACCA and the antisense primer, 5′-CTC-GAG-TCAGCTCTTAGCAGACATTGG, designed to amplify the FGF2 coding sequence, including the *Eco*RI and *Xho*I sites at the 5′ and 3′ end, respectively. By means of the *Eco*RI and *Xho*I sites, the FGF2 PCR product was incorporated into the pcDNA4 vector (Invitrogen, Carlsbad, CA), and this construct was named pcDNA-FGF2. HY-Toff-GPC3 cells were transiently transfected with pcDNA-FGF2. Cells were incubated without Dox for 48 hr and

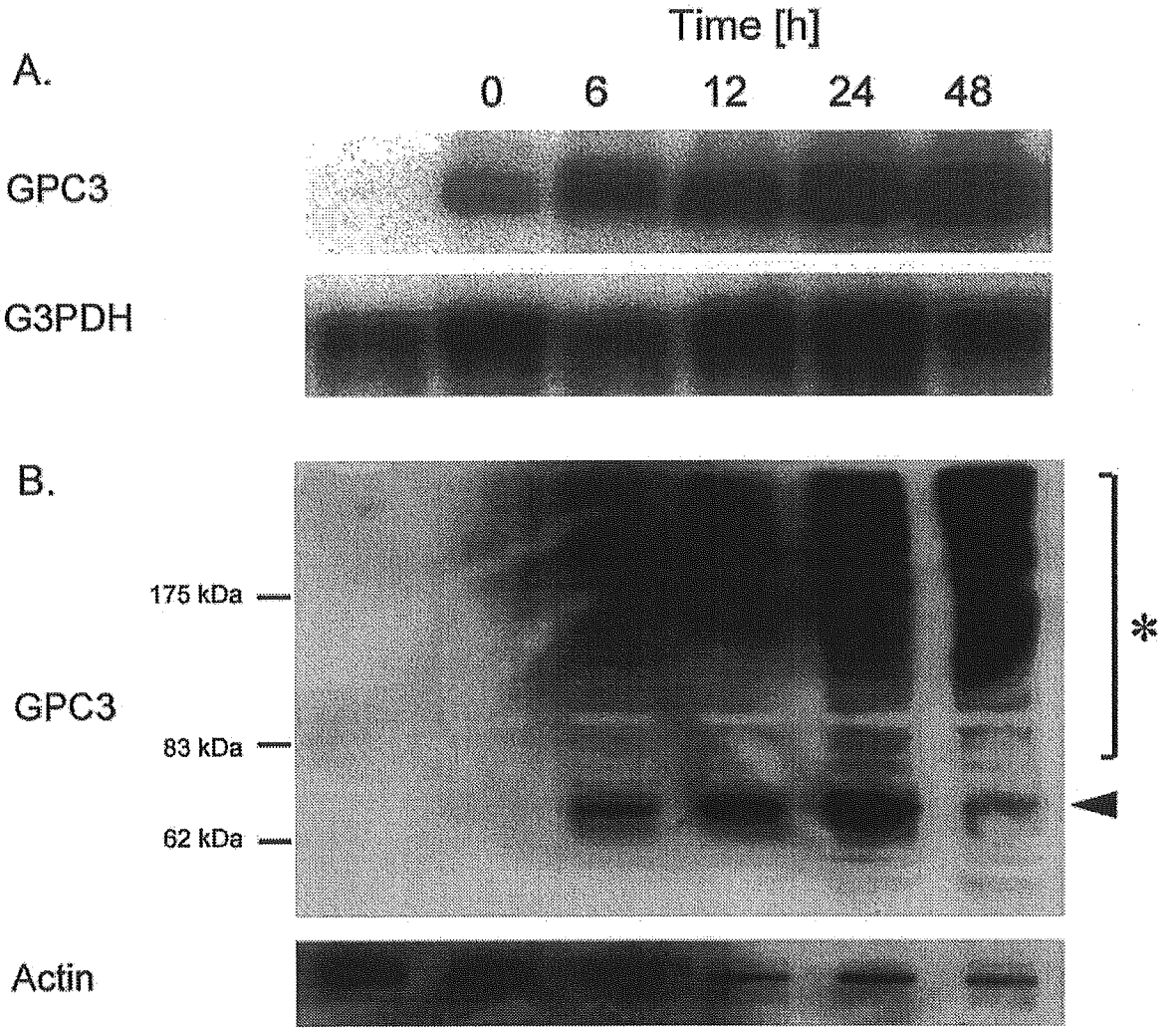

FIGURE 3 – Regulation of GPC3 expression in HY-Toff-GPC3 cells. *(a)* Northern blot analysis of the GPC3 expression level after induction by removal of Dox. The mRNA GPC3 levels elevate time-dependently, and leaky GPC3 expression was detected in the cells even without induction. The number at the top of the figure means the time after removal of Dox. Left lane, HY-Toff cells. *(b)* Western blot analysis by monoclonal anti-GPC3 antibody of the GPC3 expression levels after induction by removal of Dox. Arrowhead, core protein of GPC3; asterisk, glycosylated protein. The expression of GPC3 can be seen to increase in accordance with the GPC3 mRNA.

lysed in a lysis buffer [20 mM HEPES (pH 7.5), 150 mM NaCl, 1 mM EDTA, 10 μg/ml, 1 mM PMSF].

Interaction of GPC3 and FGF2 *in vivo* was assessed by immunoprecipitation assay. To isolate GPC3-binding FGF2 and FGF2-binding GPC3, whole-cell extracts were incubated with anti-GPC3 antibody or anti-FGF2 antibody-binding (Santa Cruz) Protein G sepharose (Amersham Pharmacia) for 1 hr with gentle rotation. After being washed with lysis buffer, the resin was boiled at 90°C with the SDS sample buffer. The supernatant was subjected to Western blot analysis to allow estimation of the interaction of FGF2 and GPC3.

Luciferase assay

The plasmid 3GC2-Lux is a luciferase reporter construct containing 3 repeats of a GC-rich sequence derived from the BMP-responsive element in the Smad6 promoter.[25] Briefly, a fragment of the mouse Smad6 gene promoter, including the BMP-responsive element was inserted into pGL2-Basic, and transcriptional activation activity was determined by luciferase assay in the presence or absence of Doxycycline using HY-Toff cells. HY-Toff cells were cotransfected with 3GC2-Lux and pRL-TK (Promega) with Tfx-20 in 6-well plates. Forty-eight hours after transfection, cells were plated at a density of 10,000 cells/well in 96-well plates with or without Dox, and BMP-7 added at various concentrations. Luciferase assay was performed using FireLite (Packard BioScience, Groningen, the Netherlands), according to the manufacturer's protocol, and luciferase activity was measured by TopCount (Packard BioScience).

Statistical analysis

The values of continuous variables are presented as the mean ± SD. The statistical analysis of the parameters collected from the 2

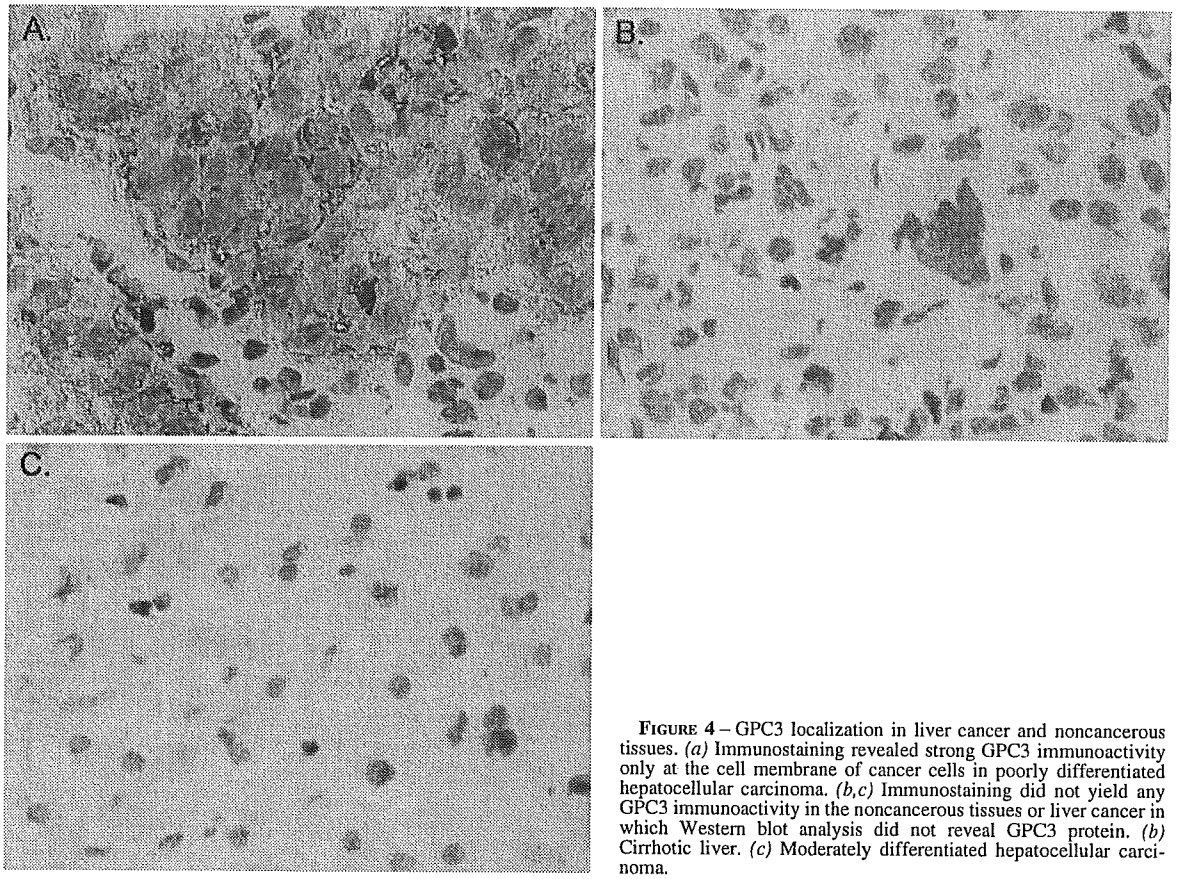

FIGURE 4 – GPC3 localization in liver cancer and noncancerous tissues. *(a)* Immunostaining revealed strong GPC3 immunoactivity only at the cell membrane of cancer cells in poorly differentiated hepatocellular carcinoma. *(b,c)* Immunostaining did not yield any GPC3 immunoactivity in the noncancerous tissues or liver cancer in which Western blot analysis did not reveal GPC3 protein. *(b)* Cirrhotic liver. *(c)* Moderately differentiated hepatocellular carcinoma.

groups, *i.e.*, the GPC3-positive and -negative groups on Western blot analysis, was determined by the χ^2 test and Student's *t*-test. Two values of the cell growth assays were compared using a 2-way factorial ANOVA test. Statistical differences were considered significant at $p < 0.05$.

RESULTS

Transcriptional expression of GPC3 by northern blot analysis

Northern blot analysis was performed on 8 liver cancer cell lines and all the tissue samples. Among the cell lines, the 2.3-kb GPC3 mRNA transcript was detected in HepG2, Hep3B, HuH6 and HuH7 at a high level and HT17, PLC/PRF/5 at a low level (Fig. 1*a*). Of the 52 tumor samples taken from 45 patients, 22 exhibited moderate to high levels of GPC3 mRNA, whereas 7 tumor samples exhibited low levels, and the intensity of the expression of GPC3 in all of these cases was higher than that in the noncancerous tissues (Fig. 2*a*). According to differentiation grade, 9 tumors exhibited the 2.3 kb GPC3 mRNA in 22 WDs (40.9%), 14 in 21 MDs (66.7%) and 6 in 9 PDs (66.7%), respectively. On the other hand, in noncancerous tissues the GPC3 mRNA was below the level of detection in all of the NL samples and was detected at a low level in 1 CH and 3 LCs (Fig. 2*a*). Therefore, the positive rates of GPC3 mRNA in HCC and chronic liver disease were 55.7% and 8.8%, respectively. Between the 2 groups, GPC3 transcript-positive or -negative of the tumor, there were no significant differences in any clinical data.

Validation of monoclonal antibody of GPC3

To confirm that the GPC3 cDNA had been cloned into the HY-Toff cells, Northern blotting was carried out with a GPC3 probe. We found that although HepG2 cells highly express endogeneous GPC3 mRNA, in the course of establishment of HY-Toff cells, these cells have lost the expression of GPC3 and the clone that does not express GPC3 has been selected (Fig. 2*a*). Zero, 6, 12, 24 and 48 hr after removing Dox, GPC3 mRNA was detectable, with the intensity dependent on the time elapsed since induction (Fig. 3*a*).

Using HY-Toff and HY-Toff-GPC3 cells, we performed Western blot analysis with an anti-GPC3 monoclonal antibody (Fig. 3*b*). Neither the 65 kDa core protein nor glycosylated protein were detected in the HY-Toff or HY-Toff-GPC3 cells with Dox, whereas a 65 kDa band did manifest in HY-Toff-GPC3 cells after the removal of Dox. The intensity of the glycosylated GPC3 protein became stronger in accordance with time after the removal of Dox, as had been the case in Northern blot analysis.

To investigate the localization of GPC3, immunohistochemical analysis with an anti-GPC3 antibody was performed on the frozen specimens (Fig. 4). Cancerous tissues in which a 65 kDa protein was detected by Western blot analysis exhibited a strong immunoactivity on the cell membrane but not in the cytoplasm or nuclei (Fig. 4*a*). In contrast, HCC without GPC3 expression on Western blot analysis and in the noncancerous tissues did not exhibit any GPC3 immunoactivity (Fig. 4*b,c*).

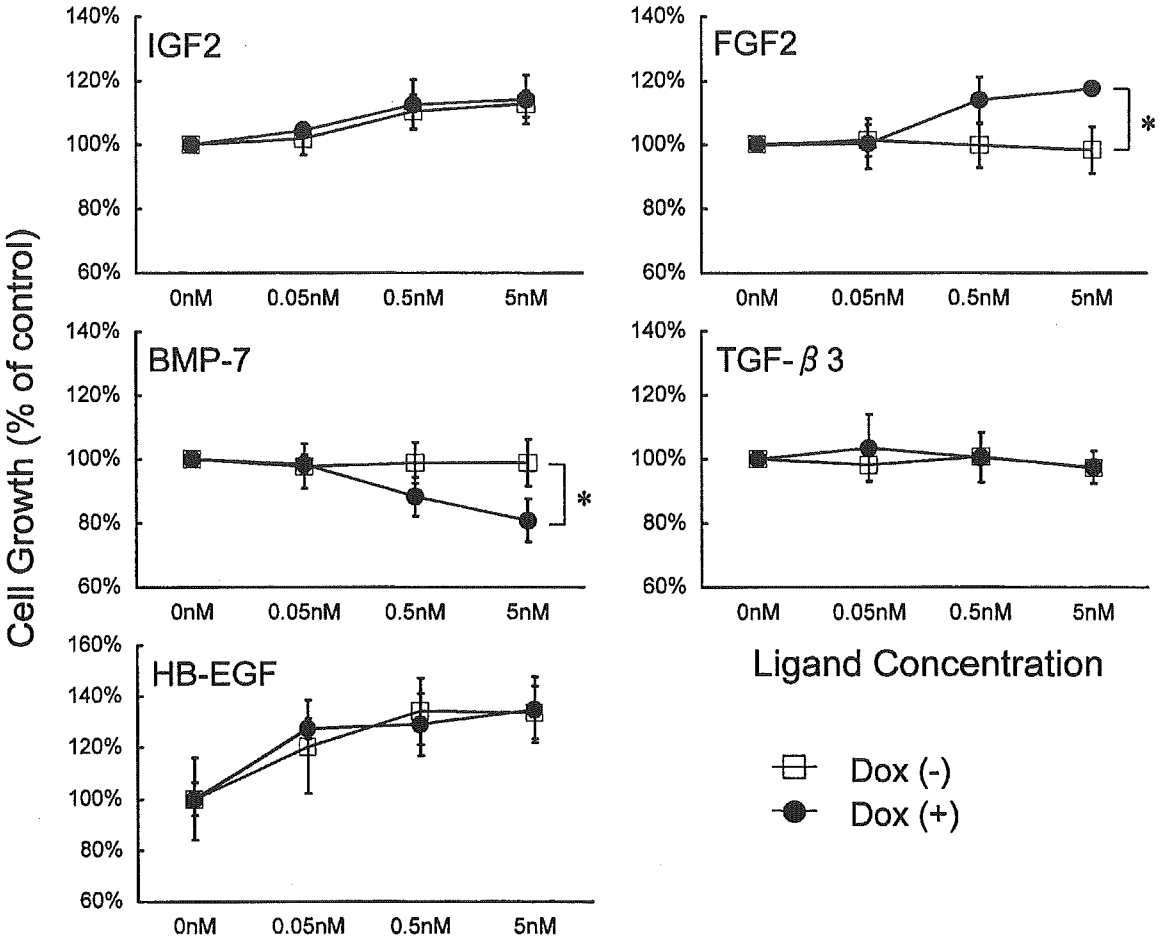

FIGURE 5 – The effects of overexpressed GPC3 on growth factor responsiveness. To keep GPC3 expression suppressed, 5 ng/ml Dox was added to the medium, and upon the removal of Dox, the expression of GPC3 was induced. HY-Toff-GPC3 cells were incubated with (filled circles) or without (open squares) Dox at the indicated concentrations of IGF2, FGF2, BMP-7, TGF-β3 and HB-EGF. Data are expressed as the percentage of change from unstimulated controls and are the mean ± SD of 3 determinations per experiment from 3 separate experiments (*$p < 0.05$).

Expression of GPC3 protein by Western blot analysis

To validate whether the GPC3-translated protein is really up-regulated in HCC, Western blot analysis was performed with the 8 HCC cell lines and all the tissue samples. Western blot analysis with an anti-GPC3 monoclonal antibody demonstrated a 65 kDa protein in 6 cell lines, HepG2, Hep3B, HT17, HuH6, HuH7 and PLC/PRF/5, and the intensity of expression was in accordance with the results of the Northern blot analysis (Fig. 1*b*). In 52 HCC cases, 15 tumors exhibited moderate to high levels of the 65 kDa band and 7 low levels (42.3%) (Fig. 2*b*). According to differentiation grade, 4 tumors exhibited the 65 kDa protein in 22 WDs (18.1%), 12 in 21 MDs (57.1%) and 6 in 9 PDs (66.7%), respectively.

On the other hand, in the noncancerous tissues, a 65 kDa band was not observed in any of the NL tissues but was detected in 1 sample of CH and 3 samples of LC at low levels (8.8%). However, in all of the noncancerous samples in which the GPC3 protein was detected by Western blot analysis, the 2.3 kb GPC3 transcript also was not detectable by Northern blot analysis (Fig. 2*b*).

To clarify the factors responsible for the positive rate of GPC3 translation, we carried out a statistical analysis that examined a variety of clinicopathologic factors including the patients' background, histologic findings in tumors and noncancerous tissues, tumor size and liver functions between the 2 groups. We found that there was only a significant difference in terms of the differentiation grade of the tumor in GPC3 protein.

Effects of GPC3 on growth factor-induced cell proliferation in HepG2 cells

First, to investigate whether enhanced expression of GPC3 can either stimulate or suppress cell growth, GPC3 was overexpressed in HY-Toff cells. However, it could not be shown that GPC3 is able to control cell proliferation in a period of up to 48 hr (data not shown). Accordingly, to determine whether enhanced expression of GPC3 regulates growth factor action, HY-Toff cells were incubated in the presence or absence of the stimulatory growth factors IGF2 or FGF2, the inhibitory growth factors BMP-7 or TGF-β and heparin-binding growth factor HB-EGF (Fig. 5). Although there was no difference in the presence or absence of overexpressed